

UC Berkeley

Research Reports

Title

Enhancements of ATMIS Using Artificial Intelligence

Permalink

<https://escholarship.org/uc/item/3fh194sj>

Authors

Liu, Henry X.
Recker, Will

Publication Date

2002-09-01

CALIFORNIA PATH PROGRAM
INSTITUTE OF TRANSPORTATION STUDIES
UNIVERSITY OF CALIFORNIA, BERKELEY

Enhancements of ATMIS Using Artificial Intelligence

Henry X. Liu, Will Recker
University of California, Irvine

**California PATH Research Report
UCB-ITS-PRR-2002-30**

This work was performed as part of the California PATH Program of the University of California, in cooperation with the State of California Business, Transportation, and Housing Agency, Department of Transportation; and the United States Department of Transportation, Federal Highway Administration.

The contents of this report reflect the views of the authors who are responsible for the facts and the accuracy of the data presented herein. The contents do not necessarily reflect the official views or policies of the State of California. This report does not constitute a standard, specification, or regulation.

Final Report for TO 4100

September 2002

ISSN 1055-1425

Enhancements of ATMIS Using Artificial Intelligence

Final Report of TO 4100

Henry X. Liu and Will Recker

California PATH ATMS Center
Institute of Transportation Studies
University of California at Irvine
Irvine, CA

Executive Summary

This report summarizes research work conducted under TO4100 at the California PATH ATMS Center at the University of California, Irvine. Under TO4100, there are three sub-projects, including:

1. TO4100-1: Capability-Enhanced PARAMICS Simulation with Developed API Library;
2. TO4100-2: Adaptive Signal Control System with On-Line Performance Measure for Single Intersection;
3. TO4100-3: An Analytical Dynamic Traffic Assignment Model with Probabilistic Travel Times and Perceptions.

These research efforts are complementary and collaborative with some ongoing and/or recently completed PATH faculty research projects at the testbed. The corresponding faculty projects are:

1. MOU 359 - Simulation of ITS on the Irvine FOT Area Using The Paramics Scalable Microscopic Traffic Simulator,
2. MOU 3008 - Field Investigation of Advanced Vehicle Reidentification Techniques and Detector Technologies, and

3. TO 4110 - Considering Risk-Taking Behavior in Travel Time Reliability.

To one extent or another, each of these existing projects addresses providing capability to Caltrans for real-time management of freeway systems – a capability that is dependent upon corresponding capability both to predict flow patterns in real-time and to adapt ramp metering and signal control strategies to meet these predicted flows.

Research summaries for each of sub-projects under TO4100 are given in the following.

1. Capability-Enhanced PARAMICS Simulation with Developed API Library

Paramics is a suite of high performance software tools used to model the movement and behavior of individual vehicles on urban and highway road networks. The Paramics Project Suite consists of Modeller, Processor, Analyzer, and Programmer. Paramics Programmer is a framework that allows the user to customize many features of underlying simulation model. Access is provided through a Functional Interface or Application Programming Interface (API).

The capability to access and modify the underlying simulation model through API is essential for research. Such an API should have a dual role, first to allow researchers to override the simulators default models, such as car following, lane changing, route choices for instance, and second, to allow them to interface complementary modules to the simulator. Complementary modules could be any ITS application, such as signal optimization, adaptive ramp metering, incident management and so on. In this way, new research ideas could be easily tested using simulator before the implementation in the real world.

We have developed a library of plug-in modules to enhance the capabilities of PARAMICS simulation through API. These API modules include actuated signal control, time-based ramp meter control, path-based routing, loop data aggregator, performance measures, MYSQL database connection, and network communication

through CORBA, etc. With these functionality enhancements, PARAMICS simulation could be customized to test and evaluate various ITS applications.

2. Adaptive Signal Control System with On-Line Performance Measure for Single Intersection

This research introduces an adaptive signal control system utilizing an on-line signal performance measure. Unlike conventional signal control systems, the proposed method employs real-time delay estimation and an on-line signal timing update algorithm. As a signal performance measure, intersection delay for each phase is measured in real-time via an advanced surveillance system that re-identifies individual vehicles both at upstream and downstream stations using vehicle waveforms obtained from advanced inductive loop detectors. In each cycle, the signal timing plan is optimized based on the delay estimated from the vehicle re-identification technology. The main thrust of the algorithm is the on-line control capability utilizing direct intersection delay measures. A description of the overall control system architecture and the optimization algorithm is addressed in this paper. Performance of the proposed system is evaluated with a high-performance microscopic traffic simulation program, Paramics, and the preliminary results have proven the promising properties of the proposed system.

3. An Analytical Dynamic Traffic Assignment Model with Probabilistic Travel Times and Perceptions

Dynamic traffic assignment (DTA) has been a topic of substantial research during the past decade. While DTA is gradually maturing, many aspects of DTA still need improvements, especially regarding its formulation and solution capabilities under the transportation environment impacted by the Advanced Transportation Management and Information Systems (ATMIS). It is necessary to develop a set of DTA models to acknowledge the fact that the traffic network itself is probabilistic and uncertain, and different classes of travelers respond differently under uncertain environment, given different levels of traffic information. This work aims to advance the state-of-the-art in

DTA modeling in the sense that the proposed model captures the travelers' decision making among discrete choices in a probabilistic and uncertain environment, in which both probabilistic travel times and random perception errors that are specific to individual travelers, are considered. Travelers' route choices are assumed to be made with the objective of minimizing perceived disutilities at each time. These perceived disutilities depend on the distribution of the variable route travel times, the distribution of individual perception errors and the individual traveler's risk taking nature at each time instant. We formulate the integrated DTA model through a variational inequality (VI) approach. Subsequently, we discuss the solution algorithm for the formulation. Experimental results are also given to verify the correctness of solutions obtained.

Table of Contents

| | |
|---|----|
| Executive Summary | I |
| Table of Contents | 1 |
| TO4100 – 1: Capability-Enhanced PARAMICS Simulation with Developed API Library | 2 |
| TO4100 – 2: Adaptive Signal Control System with On-Line Performance Measure for Single Intersection | 11 |
| TO4100 – 3: An Analytical Dynamic Traffic Assignment Model with Probabilistic Travel Times and Perceptions | 27 |

TO4100-1: ¹Capability-Enhanced PARAMICS Simulation with Developed API Library

Lianyu Chu

California PATH ATMS Testbed
Institute of Transportation Studies
University of California, Irvine
Irvine, CA 92697
Tel: 949-824-1876 Fax: 949-824-8385
Email: lchu@translab.its.uci.edu

Henry X. Liu

California PATH ATMS Testbed
Institute of Transportation Studies
University of California, Irvine
Irvine, CA 92697
Tel: 949-824-2949 Fax: 949-824-8385
Email: hliu@translab.its.uci.edu

Will Recker

Institute of Transportation Studies
University of California, Irvine
Irvine, CA 92697
Tel: 949-824-5642 Fax: 949-824-8385
Email: wwrecker@uci.edu

SUMMARY

PARAMICS is one of the widely used microscopic traffic simulation program. One important feature of PARAMICS is that PARAMICS allows the user to customize many features of underlying simulation model through a Functional Interface or Application Programming Interface (API). We have developed a library of plug-in modules to enhance the capabilities of PARAMICS simulation through API. These API modules include actuated signal control, time-based ramp meter control, path-based routing, loop data aggregator, performance measures, MYSQL database connection, and network communication through CORBA, etc. With these functionality enhancements,

¹ This paper has been accepted for presentation in the 9th ITS World Congress, Chicago, 2002.

PARAMICS simulation could be customized to test and evaluate various ITS applications.

INTRODUCTION

Simulation modeling is an increasing popular and effective tool for analyzing a wide variety of dynamical problems, which are not amendable to study by other means. Traffic simulation models can be classified as being either microscopic, mesoscopic, or macroscopic according to their representation of traffic flow (or vehicle movement). Microscopic models, such as PARAMICS, CORSIM, VISSIM, AIMSUN2, TRANSIM, MITSIM, continuously or discretely calculate and predict the state of individual vehicles, and measure the speed and location of each individual vehicle in the simulation. Macroscopic models, such as FREFLO, AUTOS, METANET, VISUM, aggregate the description of traffic flow to speed, flow, and density of each link in the network. Mesoscopic models, such as DYNASMART, DYNAMIT, INTEGRATION, METROPOLIS, have aspects of both macroscopic and microscopic models. These models have been applied successfully to particular studies, but their applications are relatively limited. Most are designed for particular applications and useful only for specific purposes, missing some components of ATMIS (1). Microscopic simulators, which do not depend on theoretical traffic flow models but on vehicle-vehicle interactions, are deemed more appropriate for evaluating various ITS applications.

PARAMICS (PARAllel MICROscopic Simulation) is a suite of microscopic simulation tools used to model the movement and behavior of individual vehicles on urban and highway road networks (2). One important feature of PARAMICS is that PARAMICS allows the user to customize and extend many features of underlying simulation model through a Functional Interface or Application Programming Interface (API). Such an API should have a dual role, first to allow researchers to override the simulators default models, such as car following, lane changing, route choices for instance, and second, to allow them to interface complementary modules to the simulator. Complementary modules could be any ITS applications, such as actuated signal control, ramp metering, VMS (Variable Message Sign) control, and so on. With these functionality enhancements, PARAMICS simulation could be customized to test and evaluate various ITS applications (3).

This paper is organized as follows. First, we will give a brief overview of California advanced traffic management system (ATMS) testbed, which is located at the University of California, Irvine. Then, the framework to enhance the functionalities of PARAMICS simulation through developed API library is given. The functions of plug-in modules in the library are described in the following. Finally, concluding remarks are presented.

CALIFORNIA ATMS TESTBED

The California ATMS Testbed at UC-Irvine is based on real-time, computer-assisted traffic management and ATM communication network. It provides an instrumented,

multi-jurisdictional, multi-agency transportation operations environment linked to university laboratories for real-world development, testing and evaluation of near-term technologies and ATMIS applications, and to serve as an ongoing testing ground for California and national ITS efforts. The testbed currently has direct links to three traffic management centers (TMCs):

- Caltrans District 12 TMC
- City of Anaheim TMC, and
- City of Irvine Transportation Research Analysis and Control Center

Real-time loop data are received at the testbed and then stored in the Oracle database. The signal control data of several major intersections in the city of Irvine are also obtained in the testbed. The signal timing can be modified through NT-based controllers by the testbed researchers. A general goal of the testbed is to develop and maintain an implementation platform that gives testbed researchers "plug and play" capabilities with ATMIS modules and sub-systems.

A microscopic traffic simulator, PARAMICS, is integrated to the testbed development environment. The prime objective of using traffic simulators in UCI ATMIS Testbed is to serve as both an off-line evaluation/design tool, and an on-line control / guidance tool for dynamic transportation management.

As a suite of ITS-capable, user-programmable, high-performance microscopic traffic simulation package, PARAMICS offers very plausible detailed modeling for many components of an 'ideal' simulator. Accurate geometry of network and smooth coding of links in PARAMICS are important for simulation results because driver's behavior relies on characteristics of drivers and vehicles, the interactions between vehicles, and network geometry as well. The ability of PARAMICS to simulate the real-world traffic has been shown by former efforts on the model calibration and validation of PARAMICS (4,5).

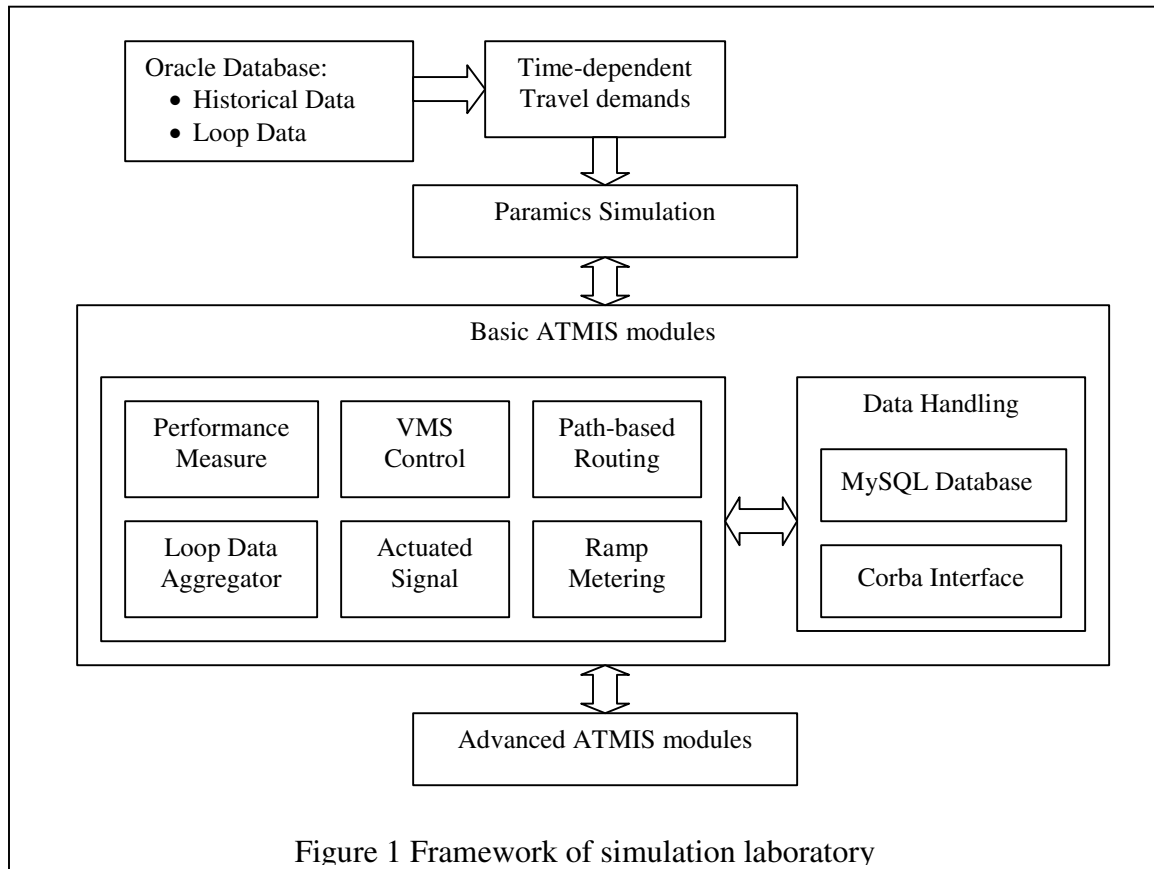
PARAMICS is fit to ATMIS research due to its high performance, scalability and the ability of modeling the emerging ITS infrastructures, such as loop detectors and VMS (6). In addition, PARAMICS provides users with API through which users can customize and extend many features of the underlying simulation model without having to deal with the underlying proprietary code.

PARAMICS in the ATMS testbed need to be customized with the following reasons:

- PARAMICS does not directly provide the control logic of ATMIS applications, which are based on the real-time data collection and data communication between on-site ITS infrastructures and local controllers or traffic management centers.
- The built-in traffic models of PARAMICS, such as car-following, routing and lane-changing models, etc. need to be replaced with some user-preferable models.

FRAMEWORK OF SIMULATION LABORATORY

The simulation laboratory is a capability-enhanced micro-simulation environment with the ability of linking simulation with the real world. The framework of the simulation laboratory is shown in Figure 1.



The core of the simulation laboratory is PARAMICS, which is regarded as a simulated traffic system with the capabilities of ITS infrastructures. The time-dependent travel demands generation module can generate time-dependent demands for PARAMICS simulations based on real-world loop data and historical travel time data stored in the database. Capability enhancements have been realized through the development of some basic ATMIS modules in PARAMICS API, including full-actuated signal controller, time-based ramp metering controller, VMS controller, path-based routing, and loop data aggregator API, that emulates the real-world data collection at a certain time interval from induction loop detectors. MYSQL database is used for storing intermediate results during the simulation process and CORBA interface is developed for the communication of different ATMIS modules.

These capability enhancements of PARAMICS constitute the API library in the testbed. An advanced ATMIS module can be further developed on top of the library. This hierarchical development of API provides the user more freedom to control the simulation processes and hence overcome some challenges faced in modeling some ITS features. As a result, various ATMIS applications can be easily tested and evaluated in

this capability-enhanced micro-simulation environment before the implementation in the real world.

CAPABILITY ENHANCEMENTS OF PARAMICS

The following API plugin modules, representing some basic ATMIS modules or user-preferred performance measures, have been developed in the testbed in order to enhance the capability of PARAMICS (7). These APIs include path-based routing, actuated signal control, time-based ramp metering control, VMS control, loop data aggregator, performance measures, etc. With these capability enhancements, the simulation laboratory is better fit to the traffic scenarios in the real world and purposes of testing and evaluating various ATMIS research and implementation projects in simulation environment.

1. Path-based Routing

PARAMICS is not a path-based but a link-based simulator. The routing information of next two links is carried by vehicles, which will decide the following route based on the routing table stored at each node along its route. The routing table is calculated based on the assignment method of the simulation, which can be specified as one of the following, all-or-nothing, stochastic or dynamic feedback.

This API controls the routing behaviors of selected vehicles by tracing them at every time step and forcing them to follow given routes. Their turning movements based on the internal routing decision should be override in order to force them to follow given routes. The route a vehicle should follow can be offline decided based on the configuration of VMS, or online decided based on a shortest path algorithm.

2. Full-actuated Signal Control

Fixed-time signal control is provided by PARAMICS. A plan/phase language is also provided to model actuated signals. However, it is difficult to be used to model the complex control logic of full-actuated signal control, widely used in California, and to replicate the logic to multiple signals.

This API implements the eight-phase, dual-ring, concurrent controller logic. The data input to this API is the signal timing plan, the geometry and detector information of each intersection. Interface functions have been provided by this API for external modules to acquire and change the default timing plan.

Based on the API module of the full-actuated signal control, the signal coordination logic is also implemented, with additional force-off logic to maintain the background cycle length and form green band for a particular phase (sync phase). This is used for emulating the signal coordination of Controller 2070.

3. Ramp Metering Control

A time-based ramp control on either a one-car-per-green basis or a n-cars-per-green basis (with $n > 1$) is implemented. The data input of this API is a time-of-day ramp control plan and the detector information of each meter. This API provided some interface functions for external modules, i.e. some advanced ramp metering algorithms, to acquire the current metering rate and set a new metering rate to a specific ramp meter.

4. Variable Message Sign Control

This API module interacts ATMIS applications with VMS signs. Through interface functions provided by this API, various ATMIS applications can dynamically update VMS information and then affect driver's behavior timely.

5. Loop Data Aggregation

PARAMICS can output two types of loop detector data for analysis:

- Point loop data, including flow, speed, headway, occupancy, and acceleration of a vehicle, and
- Link loop data, including flow, average speed, density, lane use, and lane changing on a link.

Point data is gathered at every time step when an individual vehicle passes over the loop; link data analyses the traffic data over a link, where loops locate, at a user-defined time period. However, many ATMIS applications demand point traffic data, but in an aggregated manner over user-defined time intervals, e.g. 30 seconds.

Loop data aggregator emulates the outputs of real-world data collection from induction loops, through gathering point loop data at each time step of simulation and then aggregating at any time interval specified by users. The gathered data can be raw data or smoothed data in term of user's choice. Aggregated loop data (including volume, occupancy, speed) can be output to text files or MYSQL database, and can be also accessed by interface functions defined in this API.

6. MySQL Database

A series of interface functions have been developed using MYSQL API functions for the purpose of connecting PARAMICS simulation environment with MYSQL database. This will fit to the need of storing and accessing large volume of data during the simulation process.

7. CORBA Interface

The API implements and generates a set of server objects for the relevant objects in the loaded simulation based on CORBA naming service. In this way, PARAMICS could be connected to other field device objects, or other ATMIS modules.

8. Performance Measure

PARAMICS provides a variety of measures of effectiveness (MOE) such as vehicle flow, delay, loop count, occupancy, turning counts, etc. The function of this set of performance measure APIs is to provide more user-preferable measures and some measures that cannot be provided by PARAMICS directly.

8.1 Overall Performance Measures

Due to the randomness of microscopic simulations, two measures including the average network travel time and its standard deviation are used to represent the system performance for the whole network. The average network travel time is the weighted mean of the average travel times of all OD pairs. The standard deviation of the average network travel time serves as a measure of the reliability of the network, which is the weighted standard deviation of the average travel times of all OD pairs. They are defined as

$$ATT = \frac{\sum_{\forall i,j} (T_{i,j} \cdot N_{i,j})}{\sum_{\forall i,j} N_{i,j}} \quad (1)$$

$$Std_ATT = \frac{\sum_{\forall i,j} (Std(T_{i,j}) \cdot N_{i,j})}{\sum_{\forall i,j} N_{i,j}} \quad (2)$$

where $N_{i,j}$ is the total number of vehicles that actually traveled from origin i to destination j ; $T_{i,j}$ is the average OD travel time from origin i to destination j ; $Std(T_{i,j})$ is the standard deviation of the average OD travel time from origin i to destination j .

8.2 Freeway Performance Measures

There are two parts of the freeway system, freeway mainline and entrance ramps. For the freeway mainline, we have the following two performance measures, the average speed and its standard deviation. Two loop detector stations placed on the upstream and downstream of the freeway mainline need to be specified as measurement points.

The measures for entrance ramps are the total on-ramp delay and the time percentage of the on-ramp queue spillback to the local street. These two measures are used to evaluate the effect of ramp control to the traffic flow on entrance ramps.

8.3 Arterial Performance Measures

We have two levels of performance measures for arterials. If the study is about the signal control of intersections, the performance measure we use is the intersection delay, including average stop delay, control delay, queue length of each approach, average travel time of a movement of an intersection at a certain aggregation level.

If the study is about an arterial corridor, the performance measure is the average travel time and its standard deviation between two measurement points, which can be two loop detector stations placed on the upstream and downstream of the arterial corridor.

ADVANCED ATMIS MODULES

All API modules mentioned in last section are basic ATMIS modules. An advanced ATMIS module can be an advanced ramp metering algorithm, signal optimization algorithm, or a dynamics traffic assignment algorithm, etc. The common feature of these advanced ATMIS modules is that they need to be developed based on one or more basic ATMIS API modules. This leads to a hierarchical framework of API development, which can provide the user more freedom to control the simulation processes and hence overcome some challenges faced in modeling some ITS features. As a result, various ATMIS applications can be easily tested and evaluated in this capability-enhanced micro-simulation environment before the implementation in the real world.

We have developed a set of advanced ATMIS modules about signal and ramp metering. For the signal control, multiple actuated-signal plan API and signal optimization based on real-time delay estimation algorithm have been further developed on top of the actuated signal API and intersection delay API. For the ramp metering, some advanced ramp metering algorithms have been further developed as the advanced ATMIS modules based on the ramp metering API and loop data aggregator API. These algorithms include ALINEA proposed by Papageorgiou, BOTTLENECK used in Washington State, ZONE used in Minnesota, and SWARM deployed in California.

CONCLUDING REMARKS

The capabilities of PARAMICS have been enhanced by integrating a set of API modules, including actuated signal control, time-based ramp control, loop data aggregator, Path-based routing, Performance measures, CORBA interface, and MYSQL database connection.

As a result, the customized simulation laboratory can be better fit to the traffic scenario in the real world and potentially, various ATMIS applications can be tested and evaluated in this simulation laboratory. We have used this simulation laboratory for signal optimization (8), the evaluation of adaptive ramp-metering algorithms, including the ALINEA, BOTTLENECK, ZONE, SWARM algorithms (9), and the evaluation of the effects of various ITS strategies, including traveler information, adaptive signal control, incident management, adaptive ramp metering, and their combination, under the traffic condition of year 2010.

To sum up, API programming provides users a timely solution to implement, test, and evaluate various existing or upcoming ATMIS strategies in a micro-simulator. Our practices in PARAMCIS have made PARAMICS fit to the functionality requirements of our ATMS testbed.

REFERENCES

1. Jayakrishnan, R., Oh, J., and Sahraoui A. (2001) *Calibration and Path Dynamics Issues in Microscopic simulation For Advanced Traffic Management and Information Systems*, 80th Transportation Research Board Annual Meeting, Washington D.C.
2. Smith M., S. Druitt, G. Cameron and D. MacArthur, *Paramics final Report*, Technical Report EPCC-PARAMICS-FINAL, University of Edinburgh, July, 1994.
3. Chu, L., Liu, X., Recker, W. and Zhang, H. M. (2002) *Development of A Simulation Laboratory for Evaluating Ramp Metering Algorithms*, Accepted for the presentation at TRB 2002.
4. Abdulhai, B., Sheu, J.B., and Recker, W. (1999) *Simulation of ITS on the Irvine FOT Area Using 'PARAMICS 1.5' Scalable Microscopic Traffic Simulator: Phase I: Model Calibration and Validation*, California PATH Research Report UCB-ITS-PRR-99-12, University of California, Berkeley.
5. Lee, D., Yang, X., and Chandrasekar, P. (2001) *Parameter Calibration for PARAMICS Using Genetic Algorithm*, 80th Transportation Research Board Annual Meeting, Washington D.C.
6. Algers, S., Bernauer, E., Boero, M., Breheret, L., di Taranto, C., Dougherty, M., Fox, K., and J. Gabard (1998) *Smartest Project deliverable D3*. University of Leeds.
7. Liu, X., Chu, L., and Recker, W. (2001) *PARAMICS API Design Document for Actuated Signal, Signal Coordination and Ramp Control*, California PATH Working Paper, UCB-ITS-PWP-2001-11, University of California at Berkeley, 2001.
8. Liu, X., Oh, J., Oh, S. and Chu, L. (2001) *On-line Traffic-Responsive Signal Control Scheme with Real-time Delay Estimation Technology*, Journal of East Asian Society of Transportation Studies (EASTS), Vol. 4, No. 4, pp 107-119.
9. Zhang, H. M., Kim, T., Nie, X., Jin, W., Chu, L. and Recker, W. *Evaluation of On-ramp Control Algorithm*, California PATH Research Report, UCB-ITS-PRR-2001-36.

**TO4100-2: ²ADAPTIVE SIGNAL CONTROL SYSTEM WITH ON-LINE
PERFORMANCE MEASURE FOR SINGLE INTERSECTION**

Henry X. Liu

California PATH, ATMS Center
Institute of Transportation Studies
University of California
Irvine, CA 92697

Tel: (949) 824-2949, Fax: (949) 824-8385, Email: hliu@translab.its.uci.edu

Jun-Seok Oh

Institute of Transportation Studies
University of California
Irvine, CA 92697-3600

Tel: (949) 824-1672, Fax: (949) 824-8385, Email: jsoh@uci.edu

Will Recker

Department of Civil and Environmental Engineering
Institute of Transportation Studies
University of California
Irvine, CA 92697-3600

Tel: (949) 824-5642, Fax: (949) 824-8385, Email: recker@translab.its.uci.edu

²This paper has been presented at the 81st Transportation Research Board Annual Meeting, and accepted for publication in Transportation Research Record.

Abstract:

This paper introduces an adaptive signal control system utilizing an on-line signal performance measure. Unlike conventional signal control systems, the proposed method employs real-time delay estimation and an on-line signal timing update algorithm. As a signal performance measure, intersection delay for each phase is measured in real-time via an advanced surveillance system that re-identifies individual vehicles both at upstream and downstream stations using vehicle waveforms obtained from advanced inductive loop detectors. In each cycle, the signal timing plan is optimized based on the delay estimated from the vehicle re-identification technology. The main thrust of the algorithm is the on-line control capability utilizing direct intersection delay measures. A description of the overall control system architecture and the optimization algorithm is addressed in this paper. Performance of the proposed system is evaluated with a high-performance microscopic traffic simulation program, Paramics, and the preliminary results have proven the promising properties of the proposed system.

Key Words: adaptive signal control; vehicle re-identification; intersection delay estimation; signal plan optimization

1. INTRODUCTION

A common function of a traffic control system is to seek to minimize the delay experienced by vehicles traveling through a road network of intersections by manipulating the traffic signal plans. There are various levels of sophistication in traffic signal control system applications. Basically, modes of operation can be divided into three primary categories (USDOT, 1996): pre-timed, actuated and traffic responsive. Under pre-timed operation, the master controller sets signal phases and the cycle length based on predetermined rates. These predetermined rates are determined from historical data. Common practice to develop pre-timed signal plans utilizes such offline tools as TRANSYT, which are based on traffic flows and queues observed from field data collection (McShane, 1997). Pre-timed control frequently results in the inefficient usage of intersection capacity because of the inability to adjust to variations in traffic flow and actual traffic demand; this inefficiency is pronounced when flows are substantially below capacity. An actuated controller overcomes the problem of a pre-timed controller by operating signals based on traffic demands as registered by the actuation of vehicle detectors. The green time for each approach can be varied between minimum and maximum lengths depending on flows. Cycle lengths and phases are adjusted at intervals set by vehicle actuation of loop detectors. The main feature of various actuated controllers is the ability to adjust the signal phase lengths in response to traffic flow, but attempt no systematic optimization. In the traffic responsive mode, the signal timing plan responds to current traffic conditions measured by a detection system. The general traffic responsive strategies in use are either selection of a background signal timing plan based on detector data, or online computation of a background timing plan. The computation time interval may range from one cycle length to several minutes.

With recent advances in communication network, computer, and sensor technologies, there is increasing interest in the development of traffic responsive signal control systems. Numerous systems have been proposed. The most notable of these are SCOOT (Hunt, 1982), developed in England, and SCATS (Lowrie, 1982), developed in Australia. Both SCOOT and SCATS are adaptive-cyclic systems, in that they update the signal time plan at pre-specified time intervals. Other known methods under development over the last decade include PRODYN (Henry, 1989), UTOPIA (Mauro, 1990), OPAC (Gartner, 1990), etc. These systems attempt to optimize traffic on-line without being confined to a cyclic time interval; i.e., the signal time plan may change at any time step depending on the optimization algorithm. Compared to pre-timed signal control, these systems undeniably improve overall performance in terms of total delay in the controlled network. The usual improvements amount to some 10% (Boillot, 1992).

Despite the encouraging development in adaptive signal control research in recent years and the added efficiency that has been achieved through the deployment of adaptive signal control, the prevailing lack of accurate prediction of traffic demands over the projected time horizon continues to impede the realization of substantial additional

savings. Most prediction models rely on flow data from such point detectors as conventional inductance loops, which place severe limits on the estimation of traffic variables. Because of this feature, these models cannot be modified easily for feedback real-time control schemes based on observation of variables other than flow, except indirectly (through ad-hoc prediction of queue lengths without using link flow models, for example).

This paper introduces an adaptive signal control system utilizing an on-line signal performance measure. Unlike conventional signal control systems, the proposed method employs real-time delay estimation technology and an on-line signal timing update algorithm. Intersection delay is estimated in real-time based on vehicle re-identification using an algorithm that matches individual vehicle waveforms obtained from advanced inductive loop detectors. Such vehicle re-identification technology has proven its capability to re-identify individual vehicles (Sun *et al.*, 1999) and in estimating real-time intersection delay. In this approach, the signal timing plan is optimized each cycle based on the delay estimated from the vehicle re-identification technology.

This paper is outlined as follows. The next section provides a description of the overall architecture of the signal control scheme. Section 3 presents a delay estimation scheme based on vehicle re-identification technology. Section 4 shows how the signal timing plan is optimized using the estimated delay. Section 5 evaluates the performance of the proposed method via microscopic traffic simulation experiments. Finally, Section 6 presents conclusions and future research.

2. OVERALL SYSTEM ARCHITECTURE

This section provides the overall architecture of the proposed adaptive signal control system with on-line performance measure. The system consists of five components: 1) Surveillance System, 2) Vehicle Re-identification, 3) Delay Estimation and Projection, 4) Signal Timing Optimization, and 5) Traffic Signal Controller. Figure 1 presents overall framework of the proposed adaptive signal control and connectivity of these components. The blocks above the dashed line are system blocks, which represent the operational mechanism of traffic signal systems. The blocks below the dashed line are components of the online signal optimization module that include the delay estimation via vehicle re-identification and the signal parameter optimization.

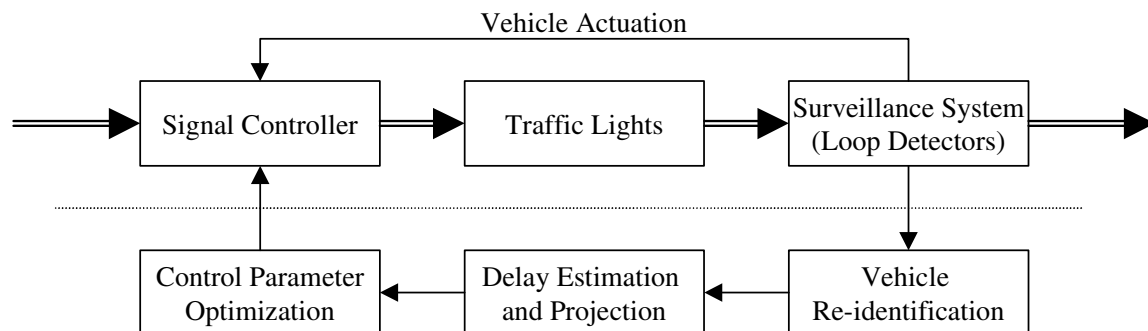


Figure 1. Overall Framework of Feedback Adaptive Signal Control

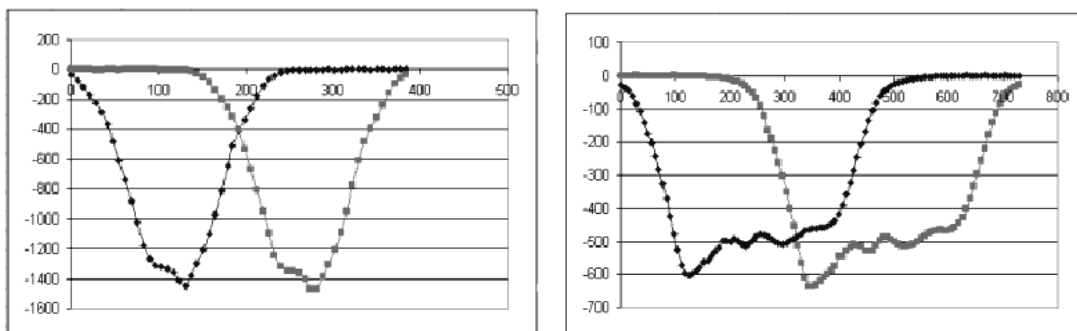
The main thrust of the proposed systems is to utilize a direct measure of delay for optimal signal control. The adaptive signal control logic attempts to directly respond to real-time demand variations from all intersections and allocates the green times on an “as needed” basis. This online signal optimization module works as a complementary module to the existing signal controller (either pre-timed or vehicle-actuated controllers) by providing optimal signal timing parameters to adapt to time-variant traffic condition.

The formulation of optimal signal control strategies requires a rich representation of the interaction between demand (i.e., vehicle arrivals) and supply (i.e., signal indications and types) at the signalized intersection. Performance estimation itself is based on assumptions regarding the characterization of the traffic arrival and service processes. It is purported herein that the direct measure of delay from vehicle re-identification can be used effectively to represent the current traffic demand. The proposed framework allows the optimization algorithm to take full advantage of this delay estimation, and provides the optimal signal timing over the projected time horizon. The optimization bears the responsibility to ensure the signal timing is consistent with control objective functions. The procedure for delay estimation and signal timing optimization is presented in next two sections.

3. REAL-TIME INTERSECTION DELAY ESTIMATION

Inductive loop detectors have been used widely both for surveillance of traffic condition and for operation of control systems. Actuated signal control systems rely on actuation of loop detectors, and adaptive control systems use measurements from the loop detectors. In this study, the loop detectors are used not only for vehicle actuation but also for delay estimation.

Detection by loop detectors is represented by a change of inductance in electric current. More detailed waveforms can be obtained using advanced loop detector cards. The waveform produces an individual vehicle’s signature that can be used for vehicle re-identification. Different types of vehicles produce correspondingly different waveforms (so-called vehicle signatures), as shown in Figure 2. Even though the same type of vehicle produces a similar form of signature, each vehicle generally has characteristics (such as number of passengers, luggage, speed, profile, etc.) that produce a locally unique signature due to differences in these characteristics. Using such characteristics, a vehicle can be re-identified from different detector stations; the time difference between the repeat signatures at two stations represents the vehicle’s travel time.



(a) Sports Car

(b) Truck

Figure 2. Typical Form of Vehicle Signature

This vehicle re-identification technology has been tested extensively at the California ATMIS Testbed at the University of California, Irvine. For vehicle signature matching, Sun *et al.* (1999) have developed a lexicographical, sequential, multi-objective optimization method. They also have shown successful performance of the loop-based vehicle re-identification on a freeway section in California. The vehicle re-identification algorithm has also been applied at the Alton/ICD (Irvine Center Drive) intersection in the city of Irvine, California. The algorithm is currently being tested at a fully instrumented signalized intersection, using upstream and downstream advanced detector stations. According to preliminary results, the algorithm can correctly match more than 40% of vehicles passing through the intersection (throughs and turns), demonstrating its online capability of intersection delay estimation.

In this study, the vehicle re-identification algorithm is used to estimate the average and total delay by movement during each cycle, and these estimates are fed to the online signal control algorithm to find the optimal green splits. The travel time for each individual vehicle is referenced to the time difference between its identification at an upstream detector and its re-identification at one of the downstream detector stations. Knowing the prevailing free speed for the approaches, and the detector distance between stations, the minimum travel time for each movement can be derived. The delay of each vehicle is calculated by deducting the minimum travel time from vehicle's actual travel time. For each cycle, each movement's delay is estimated from the measured delays of re-identified vehicles.

Because both the deterministic and random components appear together in delay projection, we employ a projection equation to suppress oscillations due to the random components as follows:

$$d(t) = \alpha_1 \cdot d^r(t) + \alpha_2 \cdot d(t-1) + \alpha_3 \cdot d(t-2) \quad (1)$$

where: $d(t)$ = filtered vehicle delay by movement

$d^r(t)$ = raw vehicle delay value from vehicle re-identification

$\alpha_1, \alpha_2, \alpha_3$ = filter coefficients in the range, and $\alpha_1 + \alpha_2 + \alpha_3 = 1$.

A signal timing plan for next time period is determined based on the projected delay. For the delay projection, filter coefficients need to be calibrated based on historical data. When α_1 equals to 1 ($\alpha_2 = \alpha_3 = 0$), the system relies on current estimation.

4. ONLINE SIGNAL CONTROL ALGORITHM

This section presents the local adaptive optimization module, including signal state description, delay estimation, mathematical formulation and computation procedures.

4.1 Signal State

A signal state at an intersection, denoted by the vector ($S(t)$), is defined by the following information: (1) the current green phase ($p(t)$), (2) the elapsed green time of current phase ($g(t)$), and (3) the vehicle delay by movements ($d(t) = [d^1, d^2, \dots, d^L]$), here L is total number of movements in the intersection. So the signal state vector is represented by:

$$S(t) = \begin{bmatrix} p(t) \\ g(t) \\ d(t) \end{bmatrix} \quad (2)$$

4.2 Control Objectives

The major considerations in the operation of an isolated intersection are: (1) safe and orderly traffic movement, (2) vehicle delay, and (3) intersection capacity. Ideally, the objectives of minimizing total delay will: (1) maximize utilization of intersection capacity, and (2) reduce the potential for accident-producing conflicts.

In this study, we consider two objectives: (1) minimization of total delay, and (2) fair treatment of each movement. The minimization of total delay, which allocates green time in favor of high demand movements, has been a well-accepted signal control objective. Such a strategy improves overall efficiency of the intersection; however, traffic from the minor approaches may suffer inordinate delay for the sake of overall system efficiency. This can result in a lengthy wait at light demand approaches. The second objective considers this fairness issue that can be caused when the system optimal strategy is applied. Based on these considerations, we adopt two-fold objective functions: the system efficiency, as represented by total vehicle delay on all approaches, and the system fairness, as represented by the standard deviation of average delay across each movement.

$$\text{System efficiency: } \min \sum_{k=1}^K \sum_{m=1}^M \sum_{n=1}^{N_m} D_n^m(k) \quad (3)$$

$$\text{System fairness: } \min \text{stdev} \left(\frac{\sum_{k=1}^K \sum_{n=1}^{N_m} D_n^m(k)}{N_m}, \forall m \right) \quad (4)$$

Where:

$D_n^m(k)$: travel delay for vehicle n in movement m at each time step k

N_m : total number of vehicles in movement m during the time horizon

M : total number of movements

K : total number of time steps

These two objectives are conflicting in their nature. A multi-objective intersection signal control is adopted that is a compromise of these two objectives, balancing the system efficiency and fairness.

4.3 Parameter Optimization

There are three primary control variables in traffic signal control: cycle length, phase sequence, and phase split. The proposed algorithm can optimize both cycle length and phase split. While cycle lengths are derived from historical traffic data, phase splits are updated every cycle based on the projected delay. The optimal cycle length can be obtained from off-line optimization based on mid-term (say, 15 minutes worth) traffic data. The crucial part of the algorithm is to adaptively seek the optimal phase split in real-time. In this paper, we consider two control policies in seeking the optimal green splits: (1) minimization of total delay, and (2) minimization of average delay. The total-delay-based on-line control is to maximize the efficiency of the system, but the fair treatment of each traffic movement is ignored. However, the average-delay-based on-line control tries to balance system efficiency and fairness in that it reduces the vehicle delays at one hand and keeps the system fair to each movement on the other, although it may gain less in terms of the system efficiency.

This adaptive control can be applied both to pre-timed signal control and actuated signal control. While the control parameter for pre-timed signal control is the green time allocated to each phase, control parameters for actuated control are initial green, minimum green, maximum green, gap, extension, etc. In the current study, for the on-line control under the actuated control system, only maximum green is used as a control variable to avoid complexity of the control problem. However, the procedures can be extended to other parameters without difficulty. The signal phase sequences follow the conventional NEMA (National Electrical Manufacturers Association) phase as in Figure 3. Numbers in the figure represents NEMA phase numbers.

In case of pre-timed control, given cycle length, we seek optimal green splits for each movement. First, we determine split between approaches (E-W and N-S) based on (total or average) delays on critical movements. Then each green split is determined proportionally. Figure 3 illustrates the proportional green split model for pre-timed signal. In this simple logic, more green time is allocated to the more congested phase.

For the actuated signal control, a similar method is applied for the maximum green allocation. Similarly, the maximum green of each phase is recalculated based on (total or average) movement delay and the background cycle length. Unlike the pre-timed case, the green time is affected by the gap and the unit extension time, so that the phase can be terminated earlier than the allocated maximum green, due to randomness in the traffic arrival pattern.

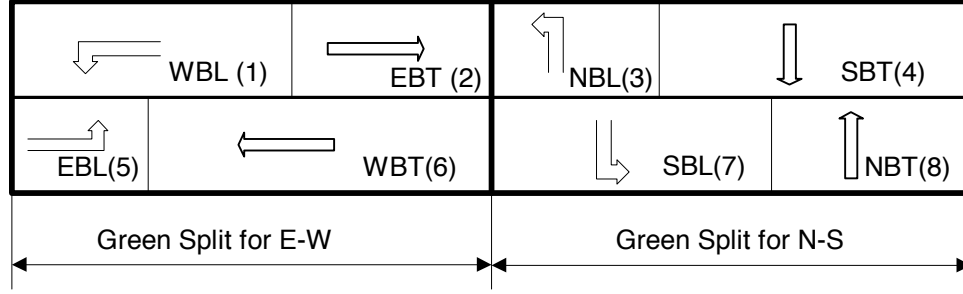


Figure 3. Proportional Green Split Model

The above method uses the current information for determining signal control in the next cycle. Although this simple method is used for the on-line adaptation of signal timing plan in this study, a more reliable system can also be designed by incorporating more complicated adaptive control logic. In feedback control applications, the most widely used form for the control algorithm is proportional/integral/derivative (PID) controller. Applying PID controller in adaptive signal control, the equation is given below:

$$G(t) = G + K_c \left[e + \frac{1}{\tau_1} \int e dt + \tau_2 \frac{de}{dt} \right] \quad (5)$$

Where, $G(t)$: current signal parameter for projected time horizon

G : bias signal parameter, is assumed to be determined by some off-line analysis and/or intuition about the historical traffic demand profile.

e : system output error, here is the difference of delay time

K_c, τ_1, τ_2 , control parameters

5. SIMULATION EXPERIMENTS

5.1 Simulation Scenario

This section compares the performance of the proposed systems via simulation experiments. The proposed system has been tested with Paramics, a high performance microscopic simulation. In this experiment, we used the on-line adaptive control model for both pre-timed signal controller and actuated signal controller. The model provides optimal green split every cycle based on the projected delay by movements. For the simple model implementation in this paper, we directly applied the estimated delay from the current cycle as the basis for determining the parameter settings for the subsequent cycle, rather than projecting one. In the experiment, two on-line control logics are applied for the green time update: total delay and average delay. A total of six cases is experimented and compared.

- 1) Pre-timed control (PTC)
- 2) On-line pre-timed control based on average delay (OPA)
- 3) On-line pre-timed control based on total delay (OPT)

- 4) Actuated control (AC)
- 5) On-line actuated control based on average delay (OAA)
- 6) On-line actuated control based on total delay (OAT)

The study site of the experiment is the intersection of Alton and Irvine Center Drive, Irvine, California, an eight phase fully actuated intersection where advanced detectors have been instrumented for a test of vehicle re-identification technology. Loop detectors are located at 325 ~ 375 feet upstream from the intersection, except for the eastbound Alton approach where detectors are located at 800 feet from the intersection. Traffic demand data were collected during p.m. peak hours from 4 to 6 p.m. The base signal timing plan for the pre-timed control was generated via SYNCHRO off-line signal timing optimization, and a set of field control parameters was adopted for the actuated signal control in this study.

5.2 Microscopic Simulation Model, Paramics (PARALLEL MICROSOPIC SIMULATION)

Paramics is a parallel, microscopic, scalable user programmable and computationally efficient traffic simulation model (Duncan 1995) that has been used in many applications in the ATMIS Testbed (Oh *et al.*, 2000). Individual vehicles are modeled in fine detail for the duration of their entire trips, providing comprehensive traffic characteristics and congestion information, as well as enabling the modeling of the interface between drivers and ITS facilities and strategies. Figure 4 shows Alton/ICD intersection in Paramics.

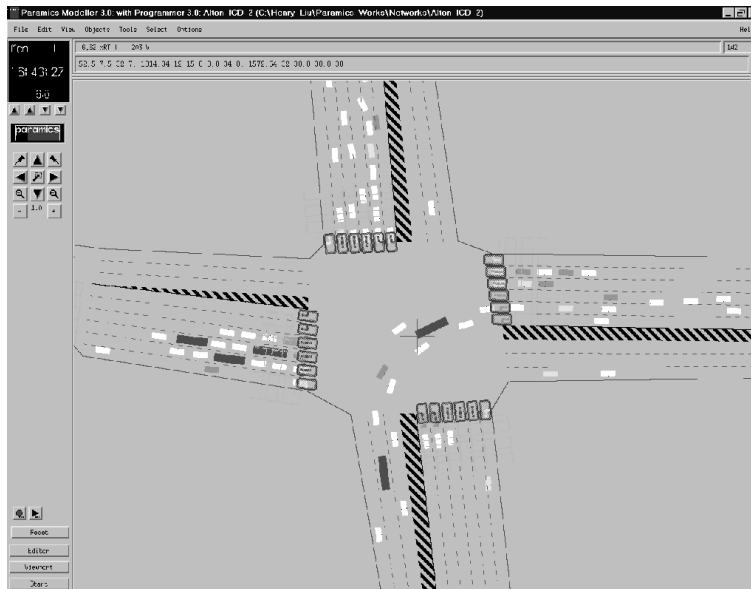


Figure 4. Alton/ICD Intersection in *Paramics*

Paramics provides a framework that allows users to customize many features of the underlying simulation model. Access is provided through a Functional Interface or Application Programming Interface (API). The capability to access and modify the underlying simulation model through API is essential for research. The APIs have a dual

role: first to allow researchers to override the simulator's default models, such as car following, lane changing, route choices for instance, and second, to allow an interface to complementary modules to the simulator. Complementary modules could be any ITS application, such as signal optimization, adaptive ramp metering, incident management and so on. In this way, new research ideas can easily be tested using the simulator before the implementation in the real world.

All of the signal control strategies employed in this study, including the fixed-time signal controller, full-actuated signal controller, and online feedback signal control with intersection delay estimation, are coded in Paramics API (Liu *et al.*, 2001).

5.3 Simulation Results

Any new or modified traffic control system should satisfy a goal or set of goals. The goals here for the proposed online signal optimization algorithm are to minimize the vehicle delay, improve the utilization of intersection capacity and reduce traffic congestion. Measures of effectiveness (MOEs) provide a quantitative basis for determining the capacity of traffic control system and their strategies to attain the desired goals. As described in Section 4.2, we consider two objectives: system efficiency and system fairness. For the system efficiency, three measures of effectiveness (MOEs) are evaluated: total intersection delay, total throughput, and average delay. The fairness of system is measured via standard deviation of movement delays.

Because Paramics is a stochastic simulation model, a Monte Carlo simulation is used to measure the system performance. A total of 30 simulation runs, each comprised of a two-hour period, were conducted for each scenario. As summarized in Table 1, the proposed on-line adaptive control outperforms both pre-timed and actuated control. Compared to the pre-timed control case, on-line control systems show greater than a 10% reduction in average delay. However, the fairness measure, standard deviation of movement delays, worsens when the total delay is used for green time update, while the control system with the average delay-based update reduces the standard deviation. That is, the average-delay-based on-line control satisfies both objectives, although the system efficiency is slightly lower than that of total delay-based on-line control.

Since the overall performance is averaged based on 30 simulation runs, the performance of the system also can be evaluated probabilistically. Figures 5, 6, 7, and 8 depict the system performance measures as probability density functions (PDF). As we can see from these figures, the average-delay-based on-line control algorithms perform better for both pre-timed and actuated signal controls. The standard deviation of the performance measure can be regarded as a measure of system stability in real application. In general, the pre-timed control systems exhibit greater stability than do the actuated control systems, and could be verified easily by the shapes of their PDF as shown in these figures.

To further detail the performance improvement under a high demand scenario, Figures 9 and 10 compare changes in average intersection delay during the two-hour simulation period, showing significant reduction of the total intersection delay.

Table 1. Comparison of Overall Performance

| MOEs | | Pre-timed Controller | | | Actuated Controller | | |
|-----------------|----------------------|----------------------|-------------------|-------------------|---------------------|--------------------|--------------------|
| | | PTC | OPA | OPT | AC | OAA | OAT |
| Efficiency | Total Delay (hrs) | 263.1 (5.5) | 238.6 (6.7) | 232.1 (4.6) | 235.9 (10.9) | 238.3 (10.5) | 231.4 (9.1) |
| | Throughput (veh) | 11072.0 (98.5) | 11284.4 (76.5) | 11057.7 (77.0) | 10772.9 (116.5) | 11250.3 (148.0) | 11011.6 (243.0) |
| | Avg. Delay (sec/veh) | 85.5 (2.0) | 76.1 (2.1) | 75.6 (1.4) | 78.8 (3.6) | 76.3 (3.5) | 75.7 (3.9) |
| Fairness | Std. of Delays | 35.0 (2.4) | 30.8 (4.1) | 40.4 (2.7) | 48.4 (3.2) | 31.4 (3.2) | 37.8 (4.7) |
| Improvement (%) | Total Delay | - | -9.3 | -11.8 | -10.3 | -9.4 | -12.0 |
| | Throughput | - | 1.9 | -0.1 | -2.7 | 1.6 | -0.5 |
| | Avg. Delay | - | -11.0 | -11.7 | -7.8 | -10.8 | -11.5 |
| | Std. of Delays | - | -11.8 | 15.4 | 38.3 | -10.2 | 8.1 |

Note: Values in () represent standard deviations of 30 simulation runs.

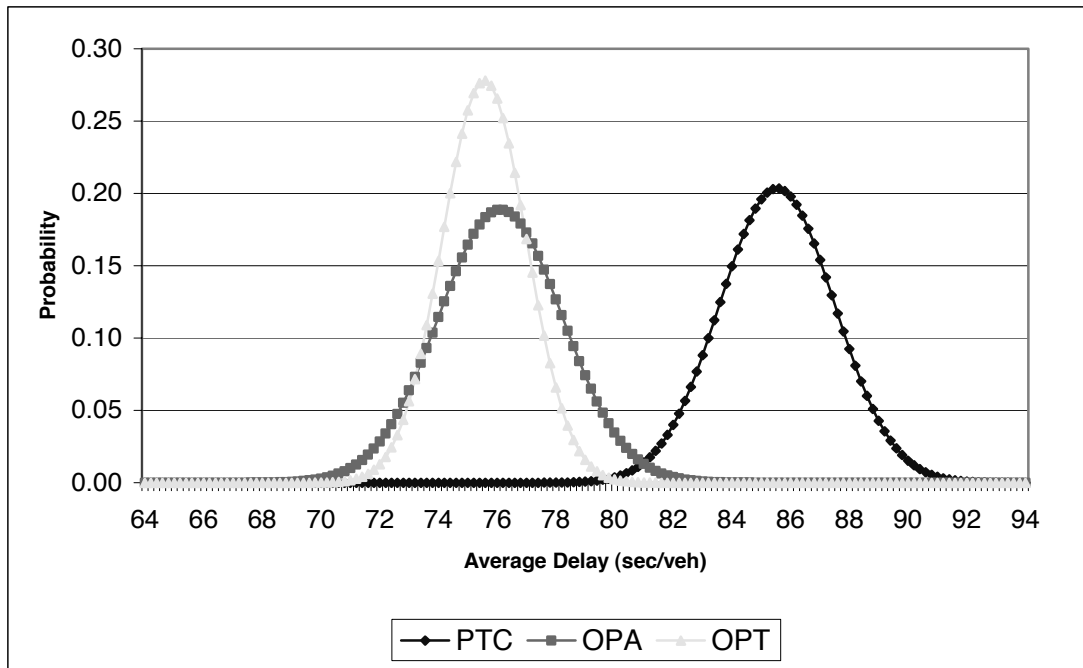


Figure 5. Probabilistic Distribution of Efficiency Measure (Pre-timed Control)

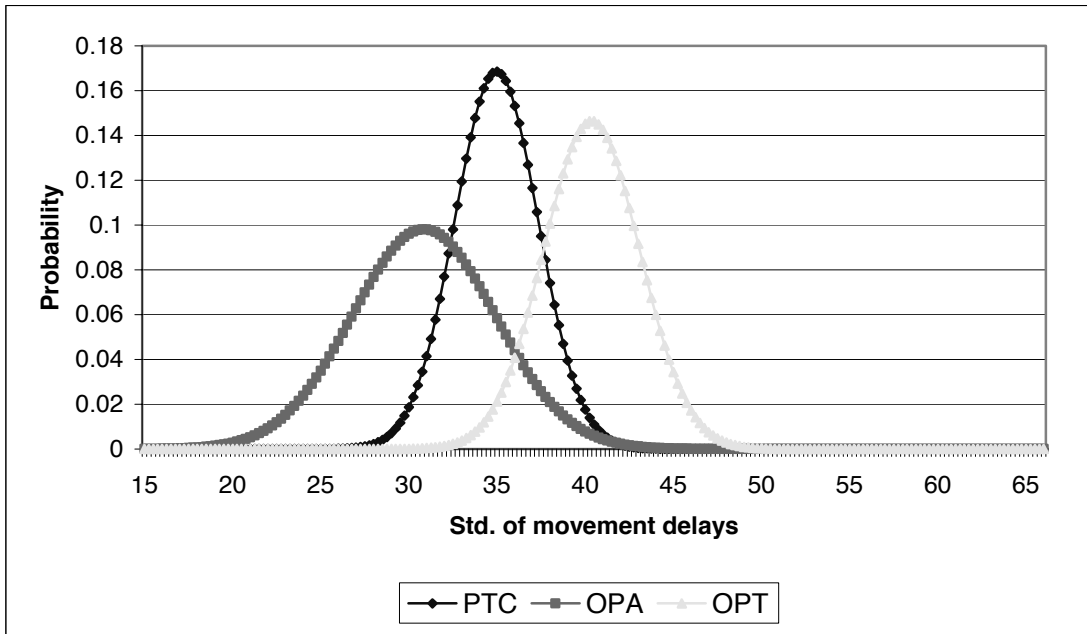


Figure 6. Probabilistic Distribution of Fairness Measure (Pre-timed Control)

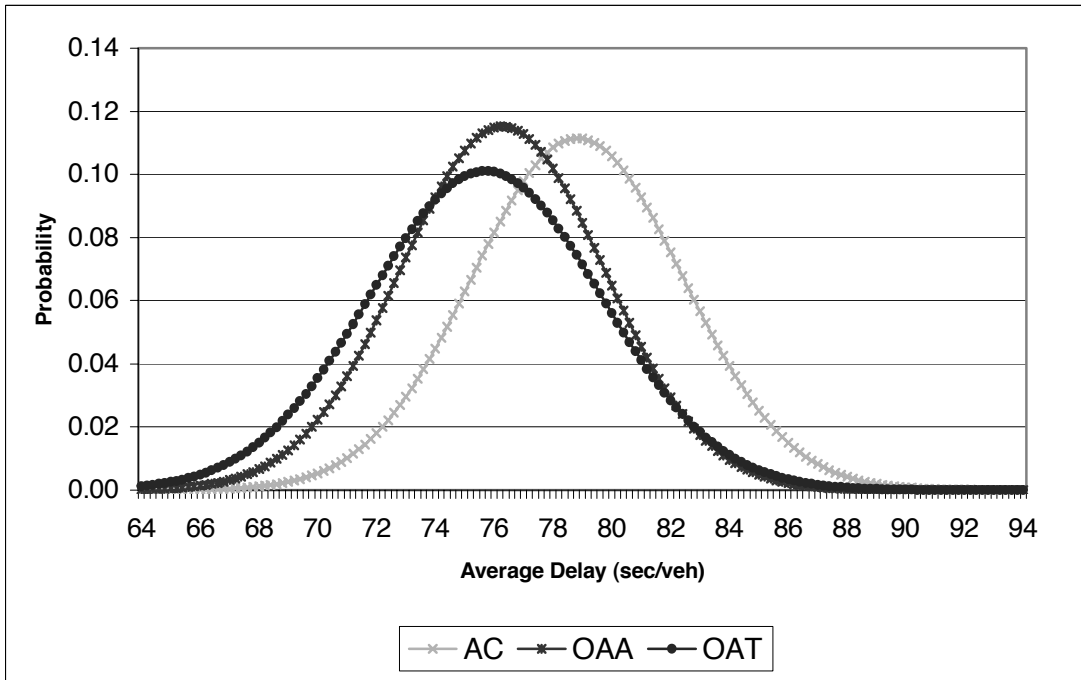


Figure 7. Probabilistic Distribution of Efficiency Measure (Actuated Control)

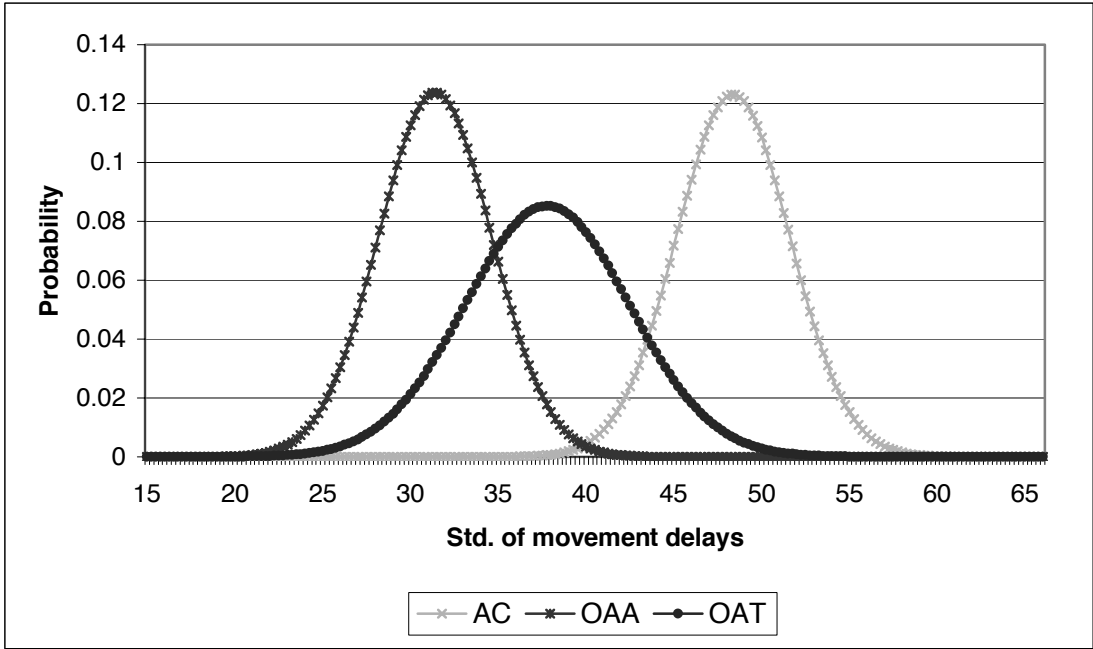


Figure 8. Probabilistic Distribution of Fairness Measure (Actuated Control)

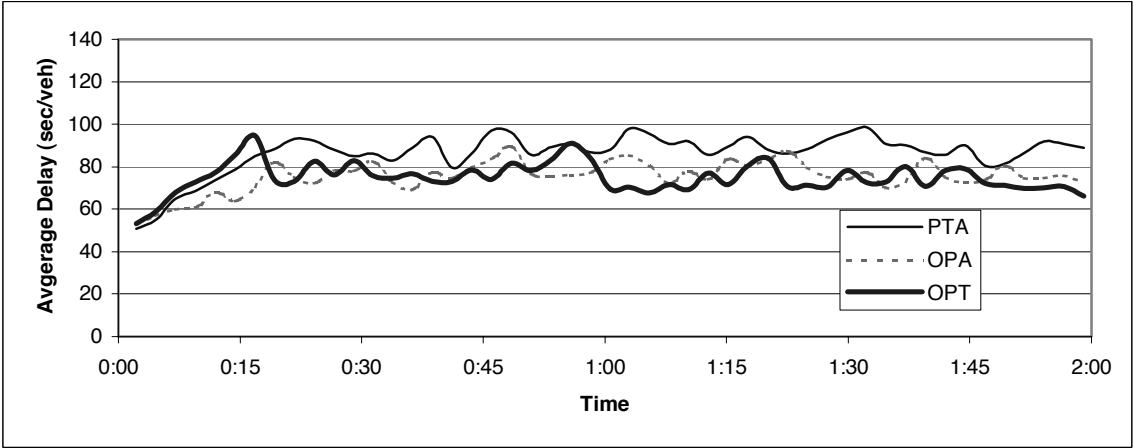


Figure 9. Comparison of Total Delay at Each Time Step (Pre-timed control)

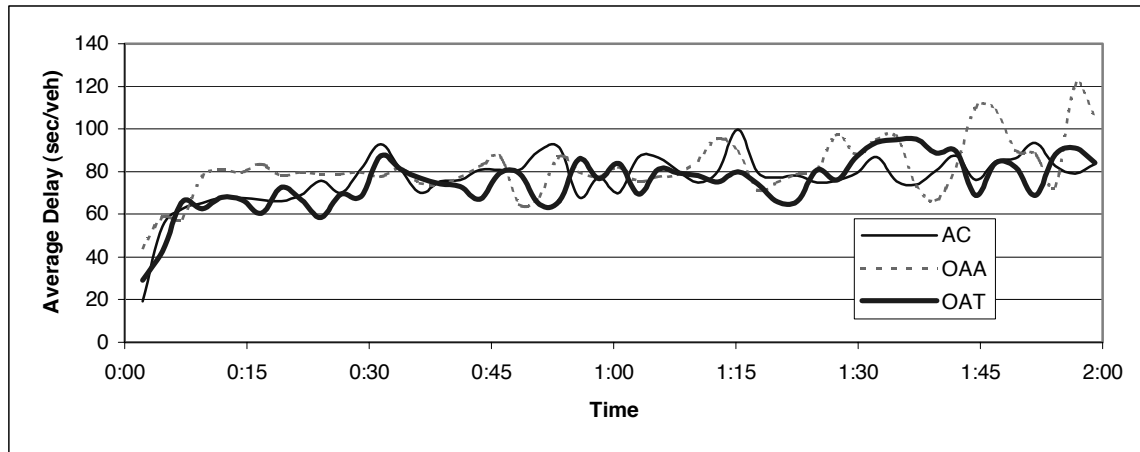


Figure 10. Comparison of Total Delay at Each Time Step (Actuated control)

6. CONCLUSIONS AND FUTURE WORK

This paper has dealt with the development of efficient techniques for the dynamic control of signalization in traffic networks in the context of Intelligent Transportation Systems. This online signal optimization module works as a complementary module to the existing signal controller for both pre-timed and vehicle actuated controllers, by providing optimal signal timing parameters. It comprises two main components: real-time delay estimation via vehicle re-identification, and on-line signal parameter optimization. We applied the on-line adaptive control system to both pre-timed and actuated control, and compared the performance of the systems via microscopic simulation model. The simulation experiments showed that the proposed adaptive control system could be an efficient method even under the application of a simple algorithm for adapting the signal timing plan.

Note that the main purpose of this paper is to present an integrated adaptive signal control algorithm with vehicle re-identification technologies. Simulation experiments were conducted on a single intersection, rather than at the network level. A natural extension of local intersection signal control is to address coordination of intersections. Specifically, coordination of the proposed adaptive controller is sought in terms of maximizing the combined performance of all of the controllers. As addressed in the paper, the performance of the system can be improved by employing more complicated control logics.

REFERENCES

Boillot, F. and Blosserville, J.M., etc. (1992) Optimal Signal Control of Urban Traffic Networks, *The 6th International Conference on Road Traffic Monitoring and Control*, IEE, England.

Duncan G.I. (1995) PARAMICS wide area micro-simulation of ATT and traffic management. *Proceedings of 28th International symposium on Automotive Technology and automation (ISATA)*, Stuttgart, Germany, pp 475-484.

Gartner, N.H. (1990) OPAC, *Control, Computers, Communications in Transportation: selected papers from the IFAC Symposium*, pp. 241-244, Pergamon Press.

Henry, J.J. and Farges, J.L. (1989) PROLYN, *Proc. of 6th IFAC-IFIP-FORS Symposium on Transportation*, pp. 505-507.

Hunt, P.B., Robertson, D.I., Bretherton, R.D., and Royle, M.C. (1982) The SCOOT online traffic signal optimization technique, *Traffic Engineering & Control* 23, pp 190-192.

Liu, X., Chu, L., Recker, W., (2001) Paramics API Design Document for Actuated Signal, Signal Coordination and Ramp Control, California PATH Working Paper, UCB-ITS-PWP-2001-11, University of California at Berkeley.

Lowrie, P.R. (1982) SCATS principles, methodologies, algorithm, *IEE Conf. On Road Traffic Signal*, IEE Publication 207, pp. 67-70, England.

Mauro V. and DiTaranto C. (1990) UTOPIA, *Control, Computers, Communications in Transportation: selected papers from the IFAC Symposium*, pp. 245-252, Pergamon Press.

McShane, W.R., Roess, R.P., and Prassas E.S. (1997) *Traffic Engineering*, second edition, Prentice Hall.

Oh, J., Cortest, C., Jayakrishnan, R., Lee, D. (2000) Microscopic Simulation with Large-network Path Dynamics for Advance Traffic Management and Information Systems. *Proceedings of 6th International Conference on Applications of Advanced Technologies in Transportation Engineering*, Singapore.

Oh, S., Oh, J., Oh, C., and Ritchie, S.G. (2001) On-Line Application of Loop-Based Vehicle Re-identification Technology to Link Travel Time and Intersection Delay Estimation, *Proceedings of the 9th World Conference on Transport Research*, Korea.

Sun, C., Ritchie, S.G., Tsai, W., and R. Jayakrishnan. (1999) Use of Vehicle Signature Analysis and Lexicographic Optimization for Vehicle Reidentification on Freeways. *Transportation Research*, Part C, Vol 7, pp 167-185.

USDOT, Federal Highway Administration (1996) *Traffic Control Systems Handbook*.

TO4100-3: ³An Analytical Dynamic Traffic Assignment Model with Probabilistic Travel Times and Perceptions

Henry X. Liu ^a, Xuegang Ban ^b, Bin Ran ^b, Pitu Mirchandani ^c

^a California PATH ATMS Center, University of California, Irvine

^b Department of Civil and Environmental Engineering, University of Wisconsin at Madison

^c Department of System Engineering, University of Arizona

ABSTRACT

Dynamic traffic assignment (DTA) has been a topic of substantial research during the past decade. While DTA is gradually maturing, many aspects of DTA still need improvements, especially regarding its formulation and solution capabilities under the transportation environment impacted by the Advanced Transportation Management and Information Systems (ATMIS). It is necessary to develop a set of DTA models to acknowledge the fact that the traffic network itself is probabilistic and uncertain, and different classes of travelers respond differently under uncertain environment, given different levels of traffic information. This paper aims to advance the state-of-the-art in DTA modeling in the sense that the proposed model captures the travelers' decision making among discrete choices in a probabilistic and uncertain environment, in which both probabilistic travel times and random perception errors that are specific to individual travelers, are considered. Travelers' route choices are assumed to be made with the objective of minimizing perceived disutilities at each time. These perceived disutilities depend on the distribution of the variable route travel times, the distribution of individual perception errors and the individual traveler's risk taking nature at each time instant. We formulate the integrated DTA model through a variational inequality (VI) approach. Subsequently, we discuss the solution algorithm for the formulation. Experimental results are also given to verify the correctness of solutions obtained.

1. INTRODUCTION

Over the past several decades, various traffic assignment models have been developed based on whether network attributes are dynamic or time-dependent, whether network stochasticity is considered in the travelers' decision making, and whether travelers' route travel time perception errors are assumed. Following Chen's classification (1) and considering both static and dynamic cases in general, traffic assignment models can be categorized as in Table 1.

Table 1. Classification of Traffic Assignment Models

| | | Accurate Perception | Inaccurate Perception |
|--------|-----------------------|---------------------|-----------------------|
| Static | Deterministic Network | DN-UE | DN-SUE |
| | Stochastic Network | SN-UE | SN-SUE |

³This paper has been presented at the 81st Transportation Research Board Annual Meeting, and accepted for publication in Transportation Research Record.

| | | | |
|---------|-----------------------|--------|---------|
| Dynamic | Deterministic Network | DN-DUO | DN-SDUO |
| | Stochastic Network | SN-DUO | SN-SDUO |

Where: DN = Deterministic Network
 SN = Stochastic Network
 UE = User Equilibrium
 SUE = Stochastic User Equilibrium
 DUO = Dynamic User Optimal
 SDUO = Stochastic Dynamic User Optimal

Among those models in Table 1, the static user equilibrium (UE) models are usually used for the long-term planning purpose (2). Most of them are formulated to be consistent with the Wardrop's first principle. This principle requires that, for used routes between a given origin-destination (OD) pair, the route cost equals the minimum route cost, and no used route has a lower cost. The basic assumption in the UE models is that over some period of time, each traveler learns and adapts to the transportation network conditions and the services available to him/her so that an equilibrium can be reached. In the DN-UE model, no network uncertainty is considered, i.e. link travel times are deterministic and each traveler is assumed to have perfect knowledge of the network travel times on all possible routes between his/her OD pair. To overcome the deficiencies of the deterministic model, DN-SUE model relaxes the assumption of travelers' perfect knowledge of network travel times, allowing travelers to select routes based on their perceived travel times. However, given that travel time uncertainty is one of the important factors in route choice as shown in a recent empirical study by Abdel-Aty et al. (7), a realistic route choice model should capture the tradeoffs between expected travel time and travel time uncertainty in decision making. The SN-SUE model falls in this category.

On the other hand, with continuous information and advice from Advanced Transportation Management and Information System (ATMIS), static UE may not exist but rather the travelers choose routes and modes based on the current perceived condition of the traffic on the network (3). Therefore, the dynamic generalization of the static UE concept is called the dynamic user optimal (DUO). One DUO traffic assignment problem is to determine vehicle flows at each instant of time on each link resulting from drivers using minimal-time routes. Thus, we are no longer considering day-to-day traffic equilibrium. Instead, we are trying to influence or control traffic and travel patterns of travelers optimally by providing accurate traffic information and effective traffic control measures. In a simple DTA model, all users of the network have perfect information on the travel times on the network and choose routes which minimize either their travel times or some generalized cost. Such a DTA model is typically deterministic. But in real life, since one might expect that network travel times for a given set of flows are stochastic in nature and also the travelers may not have perfect information about the network, the deterministic assumptions are questionable.

A large body of work is available on stochastic user equilibrium models. Dial was among the first to present the algorithm to assign link flows based on a logit model and later this stochastic user equilibrium model on deterministic networks (DN-SUE) was formulated

as an optimization problem (4). In the generalized SN-SUE model (5), proposed by Mirchandani and Soroush, the travel time on each route is random and each traveler perceives inaccurately. Thus, the perceived distribution of travel times for each traveler is a function of the actual distribution of the network travel times as well as the distribution of the traveler's own perception error. Furthermore, because it is assumed that travelers are aware of the variable nature of travel times on the network, the decision making process involved in choosing a route is assumed to represent risk taking behavior under uncertainty. Since route choice decisions usually involve tradeoffs between expected travel time and travel time uncertainty, Tatineni indicated that it may be appropriate to model travelers as either risk averse, risk prone or risk neutral, and the risk in this case is the variability associated with route travel times (6). Chen and Recker examined the effect of considering risk taking behavior in static route choice models and its impact on the estimation of travel time reliability of a road network subject to demand and supply variations (1).

In order to realize the real-time traffic network monitoring and management function in ATMIS, a SN-SDUO model that captures travelers' route choice behavior in a dynamic and stochastic transportation network needs to be developed. In this model, it is essential to understand how drivers make route choices, especially in the light of the considerable information that the driver may receive within ITS environment, such as variable message signs (VMS), highway advisory radio (HAR), and in-vehicle navigation systems, etc. Along with the driver's prior knowledge of the traffic network, such a model, as shown in Figure 1, should replicate, to the extent possible, the driver's perception of available routes and his or her decision-making in selecting the routes. Based on different assumptions on the distributions of actual route travel time and perceived route travel time error, various DTA models can be obtained. Most of current stochastic DTA models consider either a stochastic route travel time without traveler perception error such as Boyce's model (8) or deterministic network with traveler perception error such as Ran's model (9), but not both. To our knowledge, no SN-SDUO model has been proposed in the literature.

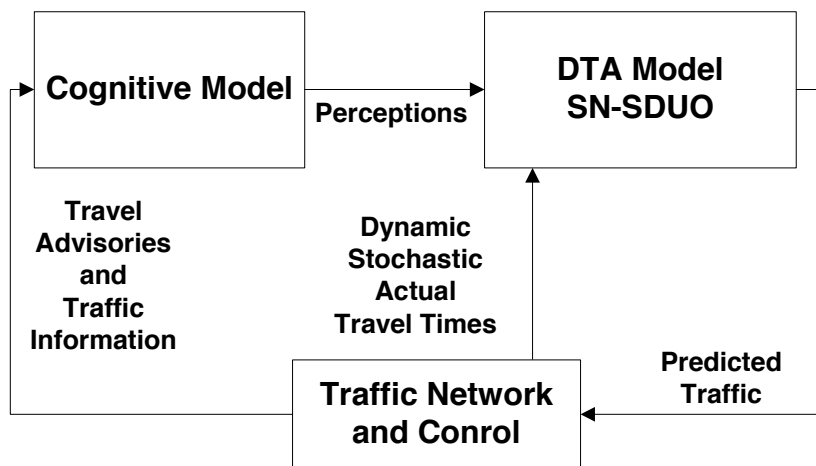


Figure 1. DTA Model with Probabilistic Travel Time and Perceptions

The objective of this paper is to propose a formulation and solution algorithm for the SN-SDUO model, which is a stochastic dynamic user optimal model based on stochastic dynamic network. This paper extends Mirchandani and Soroush’s generalized traffic equilibrium (5) into a dynamic environment. The assumption is that route travel times are variable and perceived as such by travelers at each time instant. Each traveler uses a disutility function of travel time to evaluate each route and route choices are assumed to be made with the objective of minimizing perceived disutility at each time and no traveler can reduce his/her perceived expected disutility by changing to another route. These perceived disutilities depend on the distribution of the variable route travel times, the distribution of individual perception errors, and the individual traveler’s risk taking nature at each time. By considering the traveler’s risk-taking behavior in dynamic and probabilistic environment, the proposed model can capture the traveler’s route choice characteristics such that a trade-off decision between a route with longer but reliable travel time versus another route with shorter but unreliable travel time.

This paper is organized as follows. The dynamic user-optimal route choice conditions are formulated and then a variational inequality (VI) is derived in Section 2. Traveler’s perception under dynamic and stochastic network, the stratification of traveler’s risk-taking behavior, and the route choice characteristics of these traveler classes will also be discussed in this section. In Section 3, we discuss an algorithm that can solve the VI formulation via a combination of relaxation technique, stochastic network loading, and Method of Successive Averages (MSA). Section 4 contains some computational results of applying the proposed approach to several simple scenarios, with the objective of verifying solution qualities. Finally, concluding remarks are discussed in Section 5.

2. THE VARIATIONAL INEQUALITY FORMULATION

2.1 Notation

In the following, superscript “ rs ” denotes origin-destination pair rs , subscript “ a ” (or “ b ”) denotes link a (or b), subscript “ p ” (or “ \tilde{p} ”) denotes path p (or subpath \tilde{p} between node j and destination s), and subscript “ m ” denotes traveler class m . All the variables used in the formulation are defined as follows:

- $x_a(t)$ = number of vehicles on link a at time t (main problem variable)
- $u_a(t)$ = inflow rate into link a at time t (main problem variable)
- $v_a(t)$ = exit flow rate from link a at time t (main problem variable)
- $y_a(k)$ = number of vehicles on link a at the beginning of time interval k (subproblem variable)
- $\hat{y}_a^i(k)$ = number of vehicles on link a at the beginning of time interval k at iteration i (stochastic loading loop)
- $p_a(k)$ = inflow into link a during interval k (subproblem variable)
- $\hat{p}_a^i(k)$ = inflow into link a during interval k at iteration i (stochastic loading loop)

- $q_a(k)$ = exit flow from link a during interval k (subproblem variable)
 $\hat{q}_a^i(k)$ = exit flow from link a during interval k at iteration i (stochastic loading loop)
 $f_m^{rs}(t)$ = class m departure flow rate from origin r to destination s at time t (given)
 $f_{pm}^{rs}(t)$ = class m departure flow on path p from origin r to destination s at time t
 $e^{rs}(t)$ = arrival flow rate from origin r toward destination s at time t
 $E^{rs}(t)$ = cumulative number of vehicles arriving at destination s from origin r by time t (main problem variable)
 $\bar{E}^{rs}(k)$ = cumulative number of vehicles arriving at destination s from origin r during interval k (subproblem variable)
 $A(j)$ = set of links whose tail node is j (after j)
 $B(j)$ = set of links whose head node is j (before j)
 $P_p^{rs}(t)$ = proportion of flows between (r, s) that follow route p at time t
 $\tau_a(t)$ = actual travel time over link a for flows entering link a at time t
 $\bar{\tau}_a(t)$ = estimated mean actual travel time over link a for flows entering link a at time t
 $T_a(t)$ = perceived travel time over link a for flows entering link a at time t
 $\eta_p(t)$ = actual travel time for route p between (r, s) for flows departing origin r at time t
 $\Omega_p(t)$ = perceived travel time for route p between (r, s) for flows departing origin r at time t
 $\xi_p(t)$ = perceived travel time error for route p between (r, s) for flows departing origin r at time t
 $R^{rs}(t)$ = the set of path between (r, s) at time t
 $\pi^{rs}(t)$ = minimal disutility between (r, s) for flows departing origin r at time t
 $DU_p^{rs}(t)$ = perceived disutility for route p between (r, s) for flows departing origin r at time t

2.2 Traveler's Perceptions Under Dynamic and Stochastic Network

Consider a traffic network represented by a directed graph consisting of a finite set of nodes and links. We assume that the travel times for traversing the links in the network are random variable and the probability density functions (PDF) of link travel times are dependent on the time when a link is entered. Therefore, the link travel time $\tau_a(t)$ can be modeled as a stochastic process. The stochasticity of the link travel time for a given set of flows on the traffic network could be resulted from different sources such as different weather conditions, different mix of vehicle types, and different delays experienced by different vehicles at intersections, etc. Incidents, such as vehicle breakdowns and signal failure, also contribute to the random effects of the traffic network. A network where the link travel time is modeled as a stochastic process is referred to as a dynamic and stochastic network (10).

The accuracy of a traveler perception of the network depends on the traveler's previous experience during similar network flow conditions and information available to the

traveler from various sources such as travel time updates via radio, television, internet or advanced traveler information systems. In reality, travelers may have either or both imperfect information and different perceptions towards travel time rather than perfect information and homogeneous perceptions.

Let there be M different groups of travelers, where the travelers of each group have the same disutility function and same perception error distribution. In this paper, we assume that each traveler i from group m perceives the travel time on link a of route p at time t as a distribution comprising of the distribution of actual link travel time $\tau_a(t)$ and a perception error $\xi_a^{im}(t)$, whose distribution parameters are specific to traveler i .

$$T_a^{im}(t) = \tau_a(t) + \xi_a^{im}(t), \quad a \in p, \quad p \in R^{rs}(t), \quad \forall r, s, i, m \quad (1)$$

Assume route p consists of nodes $(r, 1, 2, \dots, s)$. Then, a recursive formula for the perceived route travel time $\Omega_p^{rs}(t)$ is:

$$\Omega_p^{r1}(t) = \tau^{r1}(t) + \xi^{r1}(t) = T^{r1}(t) \quad (2)$$

...

$$\Omega_p^{rj}(t) = \Omega_p^{r(j-1)}(t) + T_a(t + \Omega_p^{r(j-1)}(t)) \quad \forall p, r, j; j = 2, \dots, s; \quad (3)$$

where link $a = (j-1, j)$. Theoretically, we will have:

$$\Omega_p^{rs}(t) = \sum_{j=1}^s T_a(t + \Omega_p^{r(j-1)}(t)) = \sum_{j=1}^s (\tau_a(t + \Omega_p^{r(j-1)}(t)) + \xi_a(t + \Omega_p^{r(j-1)}(t))) \quad \forall r, s, p \quad (4)$$

Equation (4) shows that the perceived route travel time is a random variable where the parameters of its associate probability density function (PDF) are dependent on the distribution of traveler's perception error as well as on the distribution of actual route travel time. Depending on the level of available travel time information (this includes traveler's previous knowledge) at different time period, the distribution of traveler perception error may vary dynamically. This in itself requires extensive empirical investigation; and the distribution may not be able to be represented by an algebraic function even after that. To make the model somewhat tractable, the following assumptions are made in this paper.

Assumption 1: At time instant t , the perceived error $\xi^{im}(t)$ of an individual i from group m for a segment of road with unit travel time has normal distribution $N(\mu^{im}(t), \theta^{im}(t))$.

The parameters $\mu^{im}(t)$ and $\theta^{im}(t)$ are dependent on the level of travel time information available to the traveler at time t . Therefore, we also assume:

$$\mu^{im}(t) = \mu^{im} f(\text{Info}^{im}(t), t) \quad (5)$$

$$\theta^{im}(t) = \theta^{im} g(\text{Info}^{im}(t), t). \quad (6)$$

Here, $\text{Info}^{im}(t)$ represents the available travel time information to the traveler i from group m at time t , f and g are functional relationships. The parameters μ^{im} and θ^{im} for a random individual i from group m have normal distribution $N(0, \tau^m)$ and gamma distribution

$G(\alpha^m, \beta^m)$ over the population, respectively. Here, τ^m , α^m and β^m are some constant values which are specific to group m .

Assumption 2: An individual's perceived errors are independent for non-overlapping route segments and mutually independent over the population of travelers.

Using equation (5) and (6), an individual traveler's perception error under different ATMIS scenarios can be modeled, for example, different functional relationships f and g can be used for the link with or without VMS control. Equation (5) and (6) can also capture the temporal correlation in traveler's perception error since the same tripmaker is likely to perceive travel time in a similar way from one instant to the next.

As shown by Mirchandani and Soroush (5), the moment generating function (MGF) of perceived link travel time will be used in the following section to calculate the disutility functions. Based on Equation (1), the perceived link travel time equals the sum of actual link travel time and traveler's perception error, the MGF of the perceived link travel time can be expressed as follows:

$$M_{T_a^{im}(t)}(s) = M_{\tau_a(t)}[s(1 + \mu^{im}(t) + s\theta^{im}(t)/2)] = M_{\tau_a(t)}[A] \quad (7)$$

$$\text{Here, we set } A = s(1 + \mu^{im}(t) + s\theta^{im}(t)/2). \quad (8)$$

If we assume that the actual link travel time $\tau_a(t)$ is a non-negative continuous or discrete random variable with probability density function $f_{\tau_a(t)}$, and for the ease of representation, let τ be the possible value that can be attained for the link travel time, the MGF of the perceived link travel time in Equation (7) becomes:

$$M_{T_a^{im}(t)}(s) = M_{\tau_a(t)}[A] = \int_0^{+\infty} \exp(A\tau) f_{\tau_a(t)}(\tau) d\tau \quad (9)$$

$$M_{T_a^{im}(t)}(s) = M_{\tau_a(t)}[A] = \sum \exp(A\tau) f_{\tau_a(t)}(\tau) \quad (10)$$

2.3 Traveler's Risk Taking Behavior

In everyday life, we frequently acknowledge that people have differing attitudes to risk. The shape of a utility or disutility function models a decision maker's attitude to risk. To model different types of risk taking behavior of traveler, we take the stochasticity of route travel time as the risk associated when travelers choose routes. On the basis of the perceived distribution of network travel times, travelers are assumed to behave differently when choosing routes which are probabilistic. Some are risk averse, choosing routes with longer expected travel times but lower variations. Others, the risk takers, may choose routes with shorter expected travel times but higher variations in travel time reliability.

In this paper, travelers are stratified into three classes (6), depending on their route choice behavior: (i) risk averse travelers; (ii) risk prone travelers; and (iii) risk neutral travelers. Different disutility functions are established for each class to reflect its risk-taking behavior and perceived disutilities from these functions are a function of the distribution of the variable route travel times, the distribution of individual perception errors, and the individual traveler's risk taking nature at each time. By the definitions of these disutility

functions, risk averse traveler would tend to choose routes with low expected variance of travel time, and risk prone traveler would prefer routes with highly variable travel times in an effort to shorten the journey time.

Following the study by Tatineni et al. (6), we also use the exponential disutility function, which is one of the most widely used disutility functions reported in the decision-making literature to model the different risk taking behaviors. The shapes of these different risk taking behaviors are provided in Figure 2.

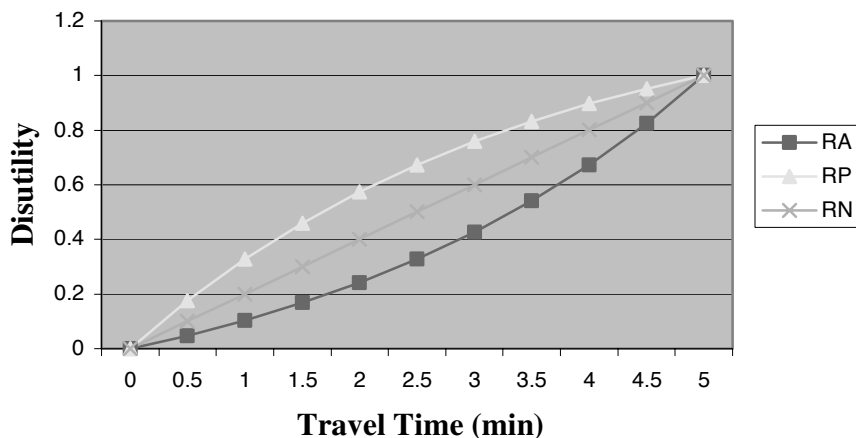


Figure 2. Disutility Functions for Different Risk-Taking Route Choice Models

To calculate the perceived expected disutility functions, the perceived route travel time is needed. A naive approach is to enumerate all paths, derive the PDF of the perceived travel time of these paths, and then compute the corresponding perceived expected disutilities. However, this could take considerable computational effort for even a small network. One important advantage of using the exponential function is that the disutility associated with a route can be estimated by summing the link disutilities on that route. This allows the classical Dijkstra-type shortest path algorithm to be used in finding the minimum expected disutility route. As discussed by Mirchandani and Soroush (5), the MGF of perceived route travel time in Equation (7) and (8) could be used to calculate the expected disutility functions, without the requirement of path enumeration. We present the results in the following. In all cases, we assume that a route with 0 minutes travel time has a disutility of 0 and a route with 5 minutes travel time has a disutility of 1. Assume route p from origin r to destination s consists of j intermediate nodes, $j = (1, 2, \dots, s)$, and link $a = (j-1, j)$ is on the route p .

For the risk averse case, the disutility function of a risk averse person takes the form of:

$$DU_p^{rs}(t) = a_1 \exp(\alpha \Omega_p^{rs}(t)) - a_2 \quad (11)$$

The perceived expected disutility function is:

$$E(DU_p^{rs}(t)) = a_1 \prod_{a \in p} M_{T_a(t + \Omega_p^{(j-1)}(t))}(\alpha) - a_2 \quad (12)$$

With the boundary conditions and the risk averse assumption, the disutility function and the perceived expected disutility function finally have the forms of:

$$DU_p^{rs}(t) = 0.309(\exp(0.289\Omega_p^{rs}(t)) - 1) \quad (13)$$

$$E(DU_p^{rs}(t)) = 0.309\left(\prod_{a \in p} M_{T_a(t+\Omega_p^{r(j-1)}(t))}(0.289) - 1\right) \quad (14)$$

For the risk prone case, the disutility function of a risk prone person takes the form of:

$$DU_p^{rs}(t) = b_2 - b_1 \exp(-\beta\Omega_p^{rs}(t)) \quad (15)$$

The perceived expected disutility function is:

$$E(DU_p^{rs}(t)) = b_2 - b_1 \prod_{a \in p} M_{T_a(t+\Omega_p^{r(j-1)}(t))}(-\beta) \quad (16)$$

With the boundary conditions and the risk averse assumption, the disutility function and the perceived expected disutility function finally have the forms of:

$$DU_p^{rs}(t) = 1.309(1 - \exp(-0.289\Omega_p^{rs}(t))) \quad (17)$$

$$E(DU_p^{rs}(t)) = 1.309(1 - \prod_{a \in p} M_{T_a(t+\Omega_p^{r(j-1)}(t))}(-0.289)) \quad (18)$$

For the risk neutral case, the disutility function is a linear function with the expected perceived travel time. For the ease of modeling, we use exponential form to approximate linear disutility function. Therefore, the disutility function of a risk neutral person takes the form of:

$$DU_p^{rs}(t) \approx c_2 - c_1 \exp(-\gamma\Omega_p^{rs}(t)) \quad (19)$$

The perceived expected disutility function is:

$$E(DU_p^{rs}(t)) \approx c_2 - c_1 \prod_{a \in p} M_{T_a(t)}(-\gamma) \quad (20)$$

With the boundary conditions and the risk neutral assumption, the disutility function and the perceived expected disutility function finally have the forms of:

$$DU_p^{rs}(t) \approx 20.5(1 - \exp(-0.01\Omega_p^{rs}(t))) \quad (21)$$

$$E(DU_p^{rs}(t)) \approx 20.5(1 - \prod_{a \in p} M_{T_a(t)}(-0.01)) \quad (22)$$

For comparison purpose, note that risk neutral travelers make route choice decisions based on the mean perceived route travel times solely, regardless the variance of perceived route travel times. Essentially, risk neutral travelers consider the route travel time as deterministic in the sense that all routes have the mean travel times. So if we assume that all travelers are risk neutral, our SN-SDUO model becomes DN-SDUO.

2.4 The Dynamic Network Constraint Set

The constraint set for our DTA problem is summarized for each class of travelers.

Route Flow Assignment Constraints:

$$f_{pm}^{rs}(t) = f_m^{rs}(t)P_p^{rs}(t) \quad \text{where } f_m^{rs}(t) \text{ is given, } \forall r, s, p; m \quad (23)$$

$$f_{pm}^{rs}(t) = u_{apm}^{rs}(t) \quad \forall r, s, p, m; a \in A(r); a \in p; \quad (24)$$

Other Constraints for all traveler classes:

Relationship between state and control variables:

$$\frac{dx_{apm}^{rs}}{dt} = u_{apm}^{rs}(t) - v_{apm}^{rs}(t) \quad \forall m, a, p, r, s \quad (25)$$

$$\frac{dE_{pm}^{rs}(t)}{dt} = e_{pm}^{rs}(t) \quad \forall p, m, r; s \neq r \quad (26)$$

Flow conservation constraints:

$$\sum_{a \in B(j)} v_{apm}^{rs}(t) = \sum_{a \in A(j)} u_{apm}^{rs}(t) \quad \forall j, p, m, r, s; j \neq r, s \quad (27)$$

$$\sum_{a \in B(s)} \sum_p v_{apm}^{rs}(t) = e_{pm}^{rs}(t) \quad \forall m, r, s; s \neq r \quad (28)$$

Flow propagation constraints:

$$x_{ap}^{rs}(t) = \sum_{b \in \tilde{p}} \{x_{bp}^{rs}[t + \tau_a(t)] - x_{bp}^{rs}(t)\} + \{E_p^{rs}[t + \tau_a(t)] - E_p^{rs}(t)\} \quad \forall a \in B(j); j \neq r; p; r, s \quad (29)$$

Definitional constraints:

$$\sum_{rspm} u_{apm}^{rs}(t) = u_a(t), \quad \sum_{rspm} v_{apm}^{rs}(t) = v_a(t), \quad \sum_{rspm} x_{apm}^{rs}(t) = x_a(t), \quad \forall a \quad (30)$$

Nonnegativity conditions:

$$x_{apm}^{rs}(t) \geq 0, \quad u_{apm}^{rs}(t) \geq 0, \quad v_{apm}^{rs}(t) \geq 0, \quad \forall m, a, p, r, s \quad (31)$$

$$f_{pm}^{rs}(t) \geq 0, \quad e_{pm}^{rs}(t) \geq 0, \quad E_{pm}^{rs}(t) \geq 0, \quad \forall p, m, r, s \quad (32)$$

Boundary conditions:

$$E_{pm}^{rs}(0) = 0, \quad \forall p, m, r, s \quad (33)$$

$$x_{apm}^{rs(0)} = 0, \quad \forall a, p, m, r, s. \quad (34)$$

For each class of travelers, the constraints expressed in (23) - (34), including flow propagation and conservation constraints, are applicable. These constraints are used to generate path and link flows when route departure flows are determined. The path departure flow $f_p^{rs}(t)$ is determined by the stochastic loading function. The link flow propagation constraints (29) are implemented for each link a , each route p , each O-D pair rs , and each time t , regardless of traveler classes. Therefore, the FIFO requirement can be ensured.

2.4 Link Travel Time and Delay Functions

Since a stochastic network is considered in this paper, variation of the link travel time should be required. Thus, in this paper, the actual link travel time $\tau_a(t)$ has two components: one is deterministic flow-dependent cruise time $c_a(t)$ and the other one is the stochastic delay $d_a(t)$. The stochastic delay may be caused by the traffic signal at the intersection for an arterial link or by the congestion for a freeway link.

There are various cruise time functions for different link types, such as freeway and arterial. To simplify the computation, it is assumed that the cruise time depends on the number of vehicles and the inflow rate. Equation (35) shows the link cruise time function chosen for the numerical results of this study:

$$c_a(t) = c_a[u_a(t), x_a(t)] = T_{a,f} [1 + \beta (\frac{u_a}{C_a} + \frac{x_a}{x_{a,max}})^\alpha] \forall a \quad (35)$$

where α and β are coefficients, $T_{a,f}$ is the free flow travel time on link a , C_a is its capacity, and $x_{a,max}$ is its maximum holding capacity.

In this paper, to simplify our algorithm, the stochastic delay is modeled as a non-negative normal distribution, which relates directly to the cruise time of this link, as shown in Equation (36).

$$d_a = N(c_a \mu_a, c_a \sigma_a^2) \quad (36)$$

where μ_a is the mean parameter and σ_a^2 is the variance parameter.

2.5 The VI Formulation

Assume travelers are disutility minimizers. The probability that route p is chosen by an individual can be stated as follows:

$$P_p^{rs}(t) = \text{Prob}(E(DU_p^{rs}(t)) \leq E(DU_q^{rs}(t))), \forall \text{ route } q \text{ between } r \text{ and } s, \forall r, s, p. \quad (37)$$

where Prob is the choice function representing the proportion of individuals who choose route p . The DUO route choice conditions are then defined as follows:

$$f_p^{rs}(t) - f^{rs}(t) P_p^{rs}(t) = 0 \quad \forall r, s, p \quad (38)$$

Note that the mean actual route travel time $\eta_p^{rs}(t)$ is increasing with path departure flow

$$f_p^{rs}(t), \text{ i.e., } \frac{\partial \eta_p^{rs}(t)}{\partial f_p^{rs}(t)} > 0 \quad \forall r, s, p \quad (39)$$

For each path p and each O-D pair rs , define an auxiliary cost term as follows:

$$F_p^{rs}(t) = [f_p^{rs}(t) - f^{rs}(t) P_p^{rs}(t)] \frac{\partial \eta_p^{rs}(t)}{\partial f_p^{rs}(t)} = 0 \quad \forall r, s, p \quad (40)$$

It is obvious that the above equality states the DUO route choice conditions, since $\partial \eta_p^{rs}(t) / \partial f_p^{rs}(t) > 0$. As shown in (11), the above system of equations is equivalent to the following variational inequality for each time instant $t \in [0, +\infty)$:

$$\sum_{rs} \sum_p F_p^{rs}(t) \{f_p^{rs}(t) - f_p^{rs*}(t)\} \geq 0 \quad (41)$$

where superscript $*$ denotes that path departure flow f has an optimal value. Since $F_p^{rs}(t) = 0$, the above inequality is also equivalent to the integral form:

$$\int_0^T \sum_{rs} \sum_p F_p^{rs}(t) \{f_p^{rs}(t) - f_p^{rs*}(t)\} dt \geq 0 \quad (42)$$

3. THE SOLUTION ALGORITHM

To solve the VI problem, we need to convert our continuous time VI problem into a discrete time VI problem. The time period $[0, T]$ is subdivided into K small time intervals. Each time interval is regarded as one unit of time. Then, $u_a(k)$ represents the inflow into link a during interval k , $v_a(k)$ represents the exit flow from link a during interval k , $x_a(k)$

represents the number of vehicles at the beginning of interval k , and $f_p(k)$ represents the departure flow from path p during interval k .

This discrete VI can be solved by using a combination of relaxation, stochastic network loading and Method of Successive Averages (MSA) techniques. In this combined algorithm, we define the travel time approximation procedure (relaxation) as the outer iteration and the MSA procedure as the inner iteration. For each relaxation (or diagonalization) iteration, we temporarily fix actual travel time $\tau_a(k)$ in link flow propagation constraints as $\bar{\tau}_a(k)$.

The algorithm for solving our proposed DTA model can be summarized as follows:

Step 0: Initialization. Initialize all link flows $\{x_{am}^{(0)}(k)\}, \{u_{am}^{(0)}(k)\}, \{v_{am}^{(0)}(k)\}$ to zero and calculate initial time estimates $\tau_a^{(1)}(k)$, regardless of traveler classes. Set the outer iteration counter $l=1$.

Step 1: Relaxation. Set the inner iteration counter $n = 1$. Find a new approximation of actual link travel times: $\bar{\tau}_a^{(n)}(k) = \tau(x_a^{(*)}(k))$, where $(*)$ denotes the final solution obtained from the most recent inner problem. Solve the route choice program for the main problem using stochastic network loading and method of successive averages.

[Step 1.1]: Subproblem - Stochastic Dynamic Network Loading. Perform Monte Carlo simulation by sampling random link travel times, calculate corresponding link disutilities. Compute minimal disutility paths and assign all departure flows $f^{rs}(k)$ to these routes during each Monte Carlo iteration. Let the temporary link flow vector resulted from the all-or-nothing loading be called $(\hat{p}^i, \hat{q}^i, \hat{y}^i)$ at Monte Carlo iteration i . Then, the stochastic dynamic network loading is solved by the following recursive equations:

$$p_a^i(k) = [(i-1)p_a^{(i-1)}(k) + \hat{p}_a^i(k)]/i \quad \forall a \quad (43)$$

$$q_a^i(k) = [(i-1)q_a^{(i-1)}(k) + \hat{q}_a^i(k)]/i \quad \forall a \quad (44)$$

$$y_a^i(k) = [(i-1)y_a^{(i-1)}(k) + \hat{y}_a^i(k)]/i \quad \forall a \quad (45)$$

Set $i = i + 1$. As i equals a prespecified number, stop. The vector (p^i, q^i, y^i) is used as the converged link flows at inner iteration n .

[Step 1.2]: Method of Successive Averages. Using the predetermined step size $1/n$, yield a new MSA main problem solution through the following equations:

$$u_a^{n+1}(k) = u_a^n(k) + \frac{1}{n}[p_a^n(k) - u_a^n(k)] \quad \forall a \quad (46)$$

$$v_a^{n+1}(k) = v_a^n(k) + \frac{1}{n}[q_a^n(k) - v_a^n(k)] \quad \forall a \quad (47)$$

$$x_a^{n+1}(k) = x_a^n(k) + \frac{1}{n}[y_a^n(k) - x_a^n(k)] \quad \forall a \quad (48)$$

If n equals a prespecified number, go to step 2; otherwise $n = n+1$, and go to step 1.1.

Step 2: Convergence Test for the Outer Iterations. If $|\bar{\tau}_a^{(l)}(k) - \bar{\tau}_a^{(l-1)}(k)| \leq \Delta$, stop. The current solution $\{u_a(k)\}, \{v_a(k)\}, \{x_a(k)\}$ is in a near optimal state; otherwise, set $l=l+1$ and go to step 1. Δ is the pre-defined threshold.

The algorithm is shown in Figure 3. The number of inner iterations n and the number of outer iterations l are correlated. If we set l large, then n should be set small and vice versa. The computational convergence of this proposed solution algorithm deserves further study.

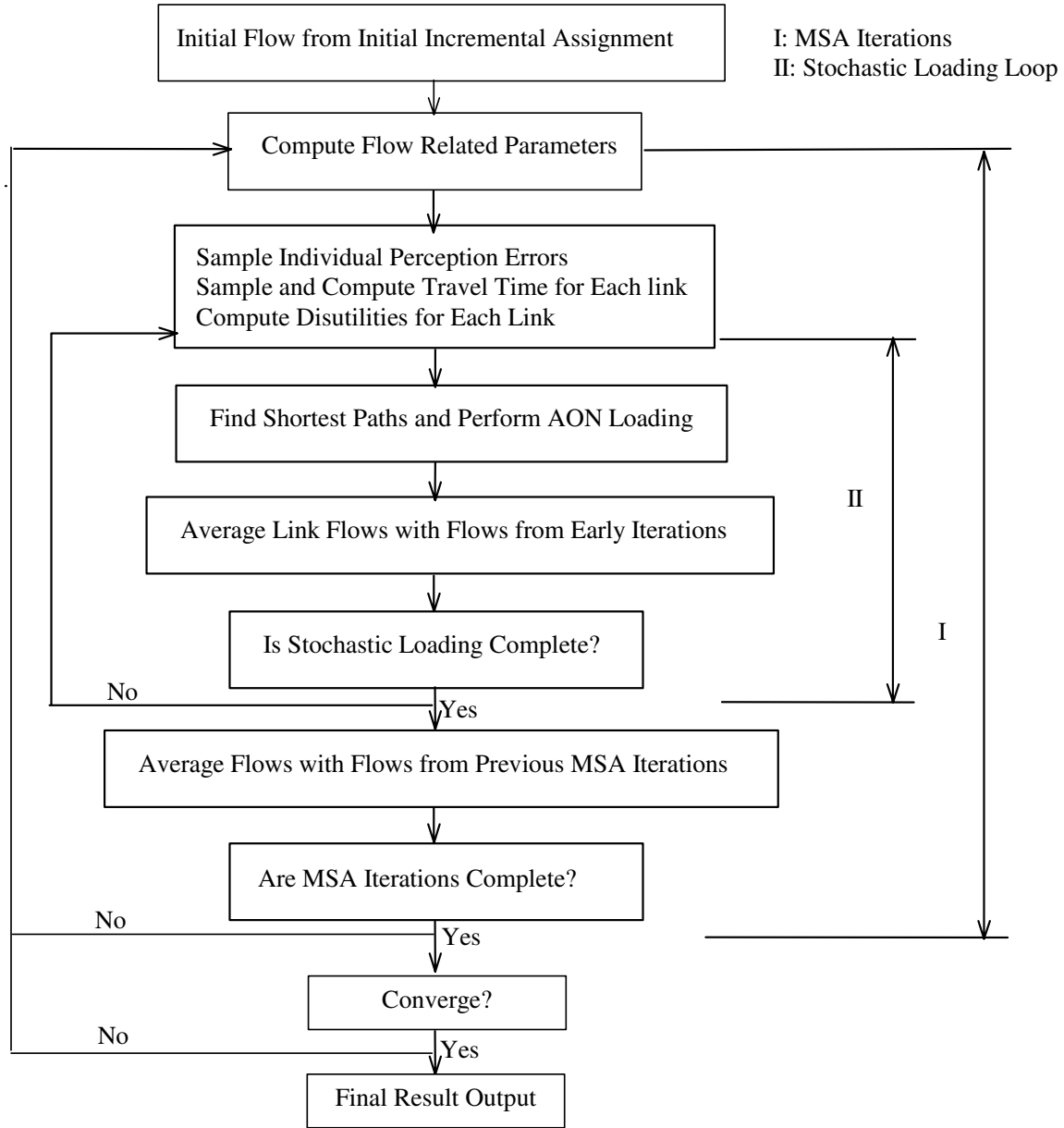


Figure 3. Solution Algorithm Flow Chart

4. EXPERIMENTAL RESULTS

In this section, we present some numerical results from our experiments for a small test network using the proposed SN-SDUO model. The objective here is not to illustrate or discuss the network performance as a function of mixed vehicle class, but merely to demonstrate solution quality. The test network is indicated in Figure 4 with seven nodes and eight links. The length of each link is 2.5 miles. Detailed link characteristics are shown in Table 2. Four scenarios, as listed in Table 3, are designed to demonstrate that the algorithm produces results that are consistent with the definitions of SN-SDUO route choices. Especially, the results from the 100% risk neutral travelers should be same with that from the DN-SDUO model. The scenarios are deliberately chosen to be simple so that one can verify the results easily. These four scenarios share the following common input characteristics:

- Origin is node 1 and destination is node 2.
- The O-D flows are 15 vehicles for each of the five 60-second periods (equivalent to a flow of 900 vehicles per hour). The total flows from Origin to Destination for the whole analysis period is 75.
- Free flow speed is 50 miles per hour.
- The delay distribution for link a is $N(c_a\mu, c_a\sigma^2)$, where c_a is the deterministic flow-dependent cruise time for link a . μ and σ^2 for each link are listed in Table 4 and shown in Figure 3.
- $\tau^m = 0.012$, $\alpha^m = 0.5$, $\beta^m = 0.01$, $m = 1,2,3$
- The Δ threshold specifying the desired accuracy was set to 0.01.

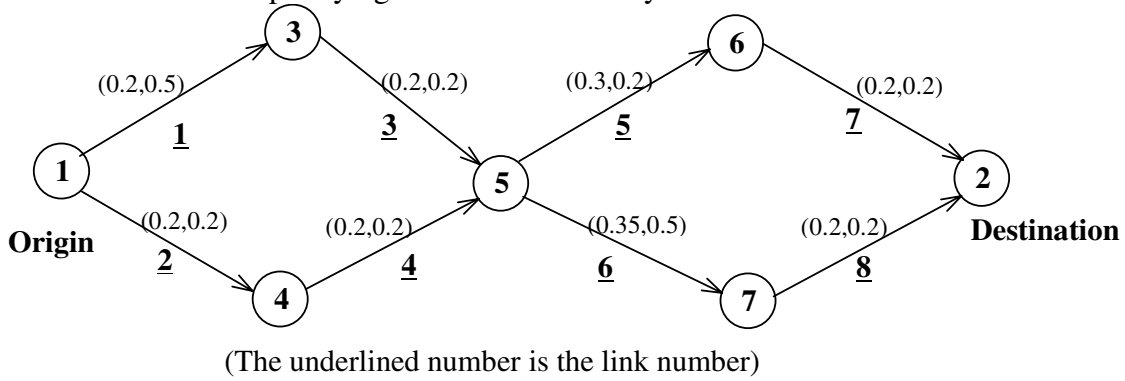


Figure 4. Experimental Network

Table 2. Link Information

| Link Number | Start Node | End Node | Length (miles) | Capacity (# of Vehi.) | # of Lane |
|-------------|------------|----------|----------------|-----------------------|-----------|
| 1 | 1 | 3 | 2.5 | 2200 | 1 |
| 2 | 1 | 4 | 2.5 | 2200 | 1 |
| 3 | 3 | 5 | 2.5 | 2200 | 1 |
| 4 | 4 | 5 | 2.5 | 2200 | 1 |
| 5 | 5 | 6 | 2.5 | 2200 | 1 |
| 6 | 5 | 7 | 2.5 | 2200 | 1 |
| 7 | 6 | 2 | 2.5 | 2200 | 1 |
| 8 | 7 | 2 | 2.5 | 2200 | 1 |

Table 3. Distinctive Features of Four Scenarios

| Scenarios | Distinctive features |
|-----------|---------------------------|
| 1 | 100% Risk Averse Traveler |

| | |
|---|----------------------------|
| 2 | 100% Risk Prone Traveler |
| 3 | 100% Risk Neutral Traveler |
| 4 | 1/3 for each group |

Table 4. Parameters of Intersection Delay for Each Link

| Link Number | Mean(μ) | Variance(σ^2) |
|-------------|---------------|------------------------|
| 1 | 0.2 | 0.5 |
| 2 | 0.2 | 0.2 |
| 3 | 0.2 | 0.2 |
| 4 | 0.2 | 0.2 |
| 5 | 0.3 | 0.2 |
| 6 | 0.35 | 0.5 |
| 7 | 0.2 | 0.2 |
| 8 | 0.2 | 0.2 |

To better present the results, we accumulate the number of vehicles passing through each link for the entire analysis period as shown in Figure 5 to Figure 8. These numbers could be verified by the time-dependent results for each link at every time interval shown as Table 5 to Table 8 in the appendix. Since the flow from origin 1 will go to node 5 and then reach destination 2, we can divide the network into two parts at node 5 and analyze them separately. Thus, links 1, 2, 3, 4 compose a sub-network and links 5, 6, 7, 8 compose another sub-network. Here we call them L-Network and R-Network, respectively.

In scenario #1, we have one group of travelers who are risk averse and their disutility function is expressed as formulation (11). For the L-Network, the intersection delay for each of the links follows normal distribution $N(0.2c_a, 0.2c_a)$ except link 1 which has a larger variance (0.5). Since the risk-averse travelers prefer route with smaller travel time variance if the means are identical, the number of travelers choosing route 1->4->5 should be more than those choosing route 1->3->5. Consequently, our algorithm assigned 58.1% (43.58 out of 75) and 41.9% (31.42 out of 75) of the total flows to these two routes, respectively. The reason that nearly 42% percent travelers still chose route 1->4->5 is because of the perception errors. For the R-Network, the intersection delay for each of the links follows normal distribution $N(0.2c_a, 0.2c_a)$ except links 5 and 6. As we have expected, 63.5% (47.64 out of 75) of the total travelers chose route 5->6->2 due to the smaller mean and variance of the intersection delay for link 5 (0.3 and 0.2, respectively) compared with link 6 (0.35 and 0.5, respectively).

In scenario #2, suppose that we have only risk-prone travelers who will prefer route with larger disutility variance given that the means are the same. Our algorithm assigned 60.7% of the travelers to route 1->3->5 and 39.3% to route 1->4->5 for the L-Network. At the same time, for the R-Network, it assigned 47.5% of the total travelers to route 5->6->2 and 52.5% to route 5->7->2. Note that, although link 6 has a larger mean (0.35) than link 5 (0.3), more travelers still chose route 5->7->2 because of the much larger variance that link 6 (0.5) has when compared with link 5 (0.2).

We consider the risk-neutral travelers in scenario #3. They will choose route mainly based on the mean of the route disutility. Therefore, our algorithm assigned the flows almost evenly to route 1->3->5(50.1%) and route 1->4->5(49.9%) because each of the four links (1,2,3,4) has the same mean (0.2). Meanwhile, for the R-Network, the mean of link 5 is smaller than that of link 6, more travelers should choose route 5->6->2 instead of route 5->7->2. This is exactly what our algorithm indicates: it assigned 55.8% of the total travelers to route 5->6->2 and 44.2% to route 5->7->2.

In scenario #4, travelers are consisted of all the three kinds of trip-makers evenly. Because the number of risk-averse travelers is just the same as that of risk-prone travelers, the risk-taking behavior of these two groups will counteract with each other to a great extent. Thus, the aggregated route-choice behavior of all the travelers in this scenario should be similar with scenario 3 in which all travelers are risk-neutral. As expected in this scenario, 50.6% and 49.4% travelers are assigned to route 1->3->5 and route 1->4->5, respectively for the L-Network, due to identical disutility mean of the four links (0.2). Whereas, a little bit more travelers (58.0%) are assigned to route 5->6->2 for the R-Network due to the smaller mean of link 5 than that of link 6.

The above analysis of experimental results from four distinctive scenarios demonstrates that our proposed analytical DTA model can fulfill the objectives of SN-SDUO, and produce realistic and reasonable dynamic traffic flow assignment for travelers traversing on a dynamic and stochastic network with different risk-taking behavior.

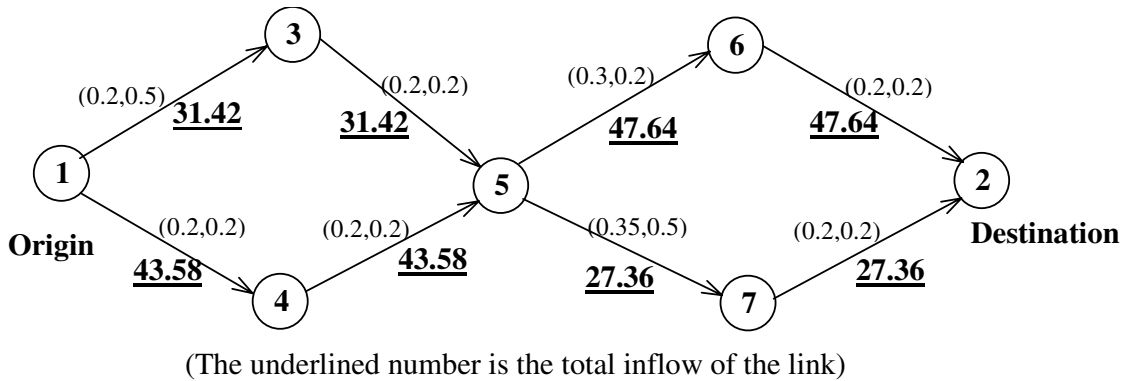
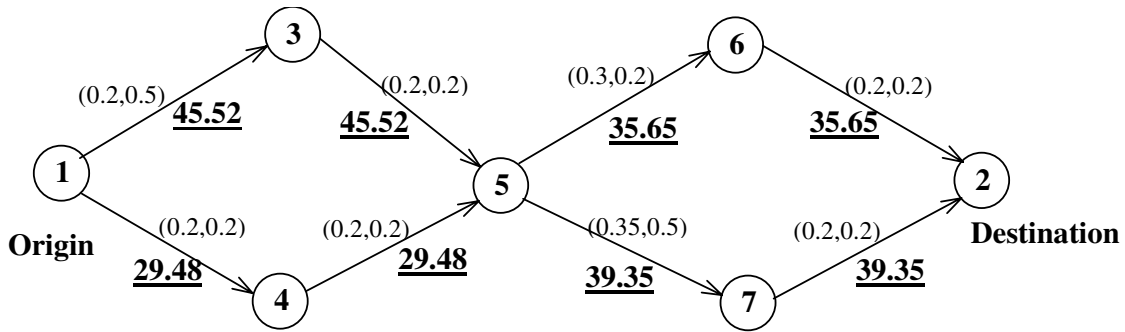
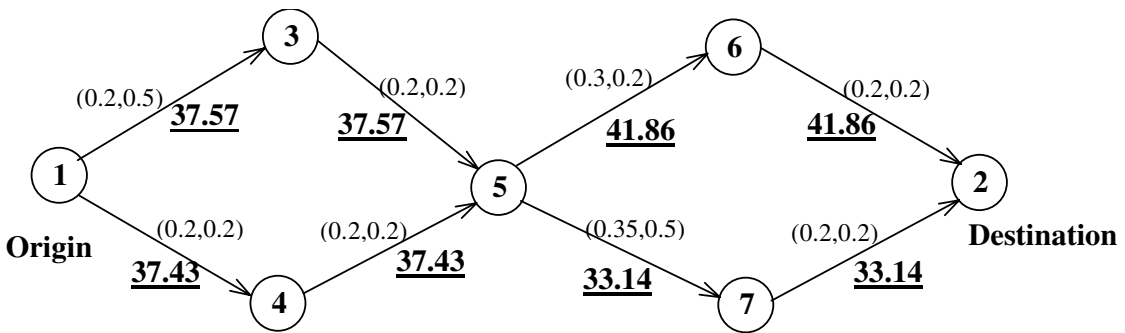


Figure 5. Results from Scenario #1



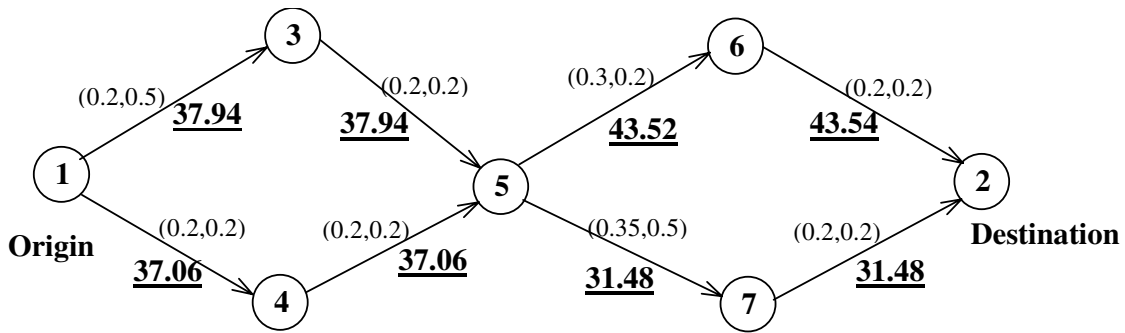
(The underlined number is the total inflow of the link)

Figure 6. Results from Scenario #2



(The underlined number is the total inflow of the link)

Figure 7. Results from Scenario #3



(The underlined number is the total inflow of the link)

Figure 8. Results from Scenario #4

5. CONCLUDING REMARKS

In this paper, we presented an analytical approach to formulate a dynamic traffic assignment model, which capture travelers' route choice behavior in a dynamic and stochastic network. Each traveler chooses a "perceived optimal route" which minimizes the perceived expected disutility of travel time from his origin node to his destination node. Our proposed model incorporates travelers' risk-taking behavior since the traffic network under consideration is stochastic. We take the stochasticity of route travel time as the risk associated when travelers choose routes. In this DTA model, three kinds of

risk-taking behavior are taken into consideration: (i) risk averse case, (ii) risk prone case, and (iii) risk neutral case. Through a variational inequality formulation, they are integrated into one modeling framework. We proposed a solution algorithm by combining a relaxation approach, stochastic network loading and method of successive averages. Four scenarios were tested to gain some computational experiences of the algorithm and to verify the solutions obtained.

The eventual goal of this effort is to develop an analytical model that can be used to examine issues and evaluate various strategies in ATMIS. A larger network consisting of both freeway links and arterial links will be used to test the model and the correctness of results will be verified in the subsequent papers. Since our model allows for the possibility that travelers may have either or both imperfect information and different perception towards probabilistic and uncertain travel time, it can be used to model the driver's perception of available routes and his or her decision-making in selecting routes under dynamic and stochastic environment, especially in the light of the considerable information that the driver may receive within ITS environment, such as variable message signs, highway advisory radio, in-vehicle navigation systems and other telematics devices. Since different information devices may have different coverage of traffic information and therefore may have different impact on traveler's route choice decision process, we will investigate and incorporate different information devices in our modeling framework for future research.

REFERENCES:

1. Chen, A. and Recker, W., (2000) *Considering Risk Taking Behavior in Travel Time Reliability*, Proceedings of 80th Transportation Research Board (TRB) Annual Meeting, Washington, D.C.
2. Sheffi, Y. (1985) *Urban Transportation Networks: Equilibrium Analysis with Mathematical Programming Methods*, Prentice-Hall, Englewoods Cliffs, New Jersey.
3. Ran, B. and Boyce, D. (1996) *Modeling dynamic transportation networks*. Springer-Verlag, Heidelberg.
4. Dial, R.B., (1971) *Probabilistic Assignment: A Multipath Traffic Assignment Model which Obviates Path Enumeration*, Transportation Research, **5**, 83-111.
5. Mirchandani, P. and Soroush, H. (1987) *Generalized Traffic Equilibrium with Probabilistic Travel Times and Perceptions*. Transportation Science, **3**, 133-151.
6. Tatineni, M., Boyce, D. E., and Mirchandani, P. (1997) Comparisons of Deterministic and Stochastic Traffic Loading Models, Transportation Research Record, 1607, 16-23.

7. Abdel-Aty, Kitamura, M. R., and Jovanis, P., (1996) *Investigating Effect of Travel Time Variability on Route Choice Using Repeated Measurement Stated Preference Data*, *Transportation Research Record*, 1493, pp.39-45.
8. Boyce, D. E., B. Ran and I. Y. Li, (1999) *Considering Travelers' Risk-Taking Behavior in Dynamic Traffic Assignment*, *Transportation Networks: Recent Methodological Advances*, M. G. H. Bell (ed.), Elsevier, Oxford, 67-81.
9. Ran, B., Lo, H. K., and Boyce, D. E., (1996) *A Formulation and Solution Algorithm for A Multi-class Dynamic Traffic Assignment Problem*, *Proceeding of the 13th International Symposium on Transportation and Traffic Theory*, Lyon, France.
10. Fu, L. and Rilett, L. R. (1998) *Expected Shortest Paths in Dynamic and Stochastic Traffic Network*, *Transportation Research B*, Vol. 32, No. 7, 499-516.
11. Nagurney, A. (1993) *Network Economics: A Variational Inequality Approach*. Kluwer Academic Publishers, Norwell, Massachusetts.

Appendix:

Table 5. Time-Dependent Flow for Scenario #1 (100% Risk Averse)

| Time Interval | Link | Flow |
|---------------|--------|-------|
| 1 | 1 -> 3 | 5.9 |
| 1 | 1 -> 4 | 9.1 |
| 2 | 1 -> 3 | 11.84 |
| 2 | 1 -> 4 | 18.16 |
| 3 | 1 -> 3 | 17.37 |
| 3 | 1 -> 4 | 27.63 |
| 4 | 1 -> 3 | 18.87 |
| 4 | 1 -> 4 | 26.13 |
| 4 | 3 -> 5 | 5.9 |
| 4 | 4 -> 5 | 9.1 |
| 5 | 1 -> 3 | 19.58 |
| 5 | 1 -> 4 | 25.42 |
| 5 | 3 -> 5 | 11.84 |
| 5 | 4 -> 5 | 18.16 |
| 6 | 1 -> 3 | 14.05 |
| 6 | 1 -> 4 | 15.95 |
| 6 | 3 -> 5 | 17.37 |
| 6 | 4 -> 5 | 27.63 |
| 7 | 1 -> 3 | 6.64 |
| 7 | 1 -> 4 | 8.36 |
| 7 | 3 -> 5 | 18.87 |
| 7 | 4 -> 5 | 26.13 |
| 7 | 5 -> 6 | 9.23 |
| 7 | 5 -> 7 | 5.77 |
| 8 | 3 -> 5 | 19.58 |
| 8 | 4 -> 5 | 25.42 |
| 8 | 5 -> 6 | 18.83 |
| 8 | 5 -> 7 | 11.17 |
| 9 | 3 -> 5 | 14.05 |
| 9 | 4 -> 5 | 15.95 |
| 9 | 5 -> 6 | 28.81 |
| 9 | 5 -> 7 | 16.19 |
| 10 | 3 -> 5 | 6.64 |
| 10 | 4 -> 5 | 8.36 |
| 10 | 5 -> 6 | 29.11 |
| 10 | 5 -> 7 | 15.89 |
| 10 | 6 -> 2 | 9.23 |
| 10 | 7 -> 2 | 5.77 |
| 11 | 5 -> 6 | 28.81 |
| 11 | 5 -> 7 | 16.19 |
| 11 | 6 -> 2 | 18.83 |
| 11 | 7 -> 2 | 11.17 |
| 12 | 5 -> 6 | 18.83 |
| 12 | 5 -> 7 | 11.17 |
| 12 | 6 -> 2 | 28.81 |
| 12 | 7 -> 2 | 16.19 |
| 13 | 5 -> 6 | 9.3 |
| 13 | 5 -> 7 | 5.7 |
| 13 | 6 -> 2 | 29.11 |
| 13 | 7 -> 2 | 15.89 |
| 14 | 6 -> 2 | 28.81 |
| 14 | 7 -> 2 | 16.19 |
| 15 | 6 -> 2 | 18.83 |
| 15 | 7 -> 2 | 11.17 |
| 16 | 6 -> 2 | 9.3 |
| 16 | 7 -> 2 | 5.7 |

Table 6. Time-Dependent Flow for Scenario #2 (100% Risk Prone)

| Time Interval | Link | Flow |
|---------------|--------|-------|
| 1 | 1 -> 3 | 9.63 |
| 1 | 1 -> 4 | 5.37 |
| 2 | 1 -> 3 | 19.24 |
| 2 | 1 -> 4 | 10.76 |
| 3 | 1 -> 3 | 27.39 |
| 3 | 1 -> 4 | 17.61 |
| 4 | 1 -> 3 | 26.59 |
| 4 | 1 -> 4 | 18.41 |
| 4 | 3 -> 5 | 9.63 |
| 4 | 4 -> 5 | 5.37 |
| 5 | 1 -> 3 | 26.28 |
| 5 | 1 -> 4 | 18.72 |
| 5 | 3 -> 5 | 19.24 |
| 5 | 4 -> 5 | 10.76 |
| 6 | 1 -> 3 | 18.13 |
| 6 | 1 -> 4 | 11.87 |
| 6 | 3 -> 5 | 27.39 |
| 6 | 4 -> 5 | 17.61 |
| 7 | 1 -> 3 | 9.3 |
| 7 | 1 -> 4 | 5.7 |
| 7 | 3 -> 5 | 26.59 |
| 7 | 4 -> 5 | 18.41 |
| 7 | 5 -> 6 | 6.98 |
| 7 | 5 -> 7 | 8.02 |
| 8 | 3 -> 5 | 26.28 |
| 8 | 4 -> 5 | 18.72 |
| 8 | 5 -> 6 | 13.78 |
| 8 | 5 -> 7 | 16.22 |
| 9 | 3 -> 5 | 18.13 |
| 9 | 4 -> 5 | 11.87 |
| 9 | 5 -> 6 | 20.23 |
| 9 | 5 -> 7 | 24.77 |
| 10 | 3 -> 5 | 9.3 |
| 10 | 4 -> 5 | 5.7 |
| 10 | 5 -> 6 | 21.52 |
| 10 | 5 -> 7 | 23.48 |
| 10 | 6 -> 2 | 6.98 |
| 10 | 7 -> 2 | 8.02 |
| 11 | 5 -> 6 | 21.87 |
| 11 | 5 -> 7 | 23.13 |
| 11 | 6 -> 2 | 13.78 |
| 11 | 7 -> 2 | 16.22 |
| 12 | 5 -> 6 | 15.42 |
| 12 | 5 -> 7 | 14.58 |
| 12 | 6 -> 2 | 20.23 |
| 12 | 7 -> 2 | 24.77 |
| 13 | 5 -> 6 | 7.16 |
| 13 | 5 -> 7 | 7.84 |
| 13 | 6 -> 2 | 21.52 |
| 13 | 7 -> 2 | 23.48 |
| 14 | 6 -> 2 | 21.87 |
| 14 | 7 -> 2 | 23.13 |
| 15 | 6 -> 2 | 15.42 |
| 15 | 7 -> 2 | 14.58 |
| 16 | 6 -> 2 | 7.16 |
| 16 | 7 -> 2 | 7.84 |

Table 7. Time-Dependent Flow for Scenario #3 (100% Risk Neutral)

| Time Interval | Link | Flow |
|---------------|--------|-------|
| 1 | 1 -> 3 | 7.78 |
| 1 | 1 -> 4 | 7.22 |
| 2 | 1 -> 3 | 15.71 |
| 2 | 1 -> 4 | 14.29 |
| 3 | 1 -> 3 | 23.05 |
| 3 | 1 -> 4 | 21.95 |
| 4 | 1 -> 3 | 22.48 |
| 4 | 1 -> 4 | 22.52 |
| 4 | 3 -> 5 | 7.78 |
| 4 | 4 -> 5 | 7.22 |
| 5 | 1 -> 3 | 21.87 |
| 5 | 1 -> 4 | 23.13 |
| 5 | 3 -> 5 | 15.71 |
| 5 | 4 -> 5 | 14.29 |
| 6 | 1 -> 3 | 14.52 |
| 6 | 1 -> 4 | 15.48 |
| 6 | 3 -> 5 | 23.05 |
| 6 | 4 -> 5 | 21.95 |
| 7 | 1 -> 3 | 7.32 |
| 7 | 1 -> 4 | 7.68 |
| 7 | 3 -> 5 | 22.48 |
| 7 | 4 -> 5 | 22.52 |
| 7 | 5 -> 6 | 8.31 |
| 7 | 5 -> 7 | 6.69 |
| 8 | 3 -> 5 | 21.87 |
| 8 | 4 -> 5 | 23.13 |
| 8 | 5 -> 6 | 16.34 |
| 8 | 5 -> 7 | 13.66 |
| 9 | 3 -> 5 | 14.52 |
| 9 | 4 -> 5 | 15.48 |
| 9 | 5 -> 6 | 24.76 |
| 9 | 5 -> 7 | 20.24 |
| 10 | 3 -> 5 | 7.32 |
| 10 | 4 -> 5 | 7.68 |
| 10 | 5 -> 6 | 24.9 |
| 10 | 5 -> 7 | 20.1 |
| 10 | 6 -> 2 | 8.31 |
| 10 | 7 -> 2 | 6.69 |
| 11 | 5 -> 6 | 25.52 |
| 11 | 5 -> 7 | 19.48 |
| 11 | 6 -> 2 | 16.34 |
| 11 | 7 -> 2 | 13.66 |
| 12 | 5 -> 6 | 17.1 |
| 12 | 5 -> 7 | 12.9 |
| 12 | 6 -> 2 | 24.76 |
| 12 | 7 -> 2 | 20.24 |
| 13 | 5 -> 6 | 8.65 |
| 13 | 5 -> 7 | 6.35 |
| 13 | 6 -> 2 | 24.9 |
| 13 | 7 -> 2 | 20.1 |
| 14 | 6 -> 2 | 25.52 |
| 14 | 7 -> 2 | 19.48 |
| 15 | 6 -> 2 | 17.1 |
| 15 | 7 -> 2 | 12.9 |
| 16 | 6 -> 2 | 8.65 |
| 16 | 7 -> 2 | 6.35 |

Table 8. Time-Dependent Flow for Scenario #4 (1/3 for each group)

| Time Interval | Link | Flow (Averse) | Flow (Neutral) | Flow (Prone) | Flow (Total) |
|---------------|-------|---------------|----------------|--------------|--------------|
| 1 | 1 → 3 | 2.12 | 2.6 | 3.1 | 7.82 |
| 1 | 1 → 4 | 2.88 | 2.4 | 1.9 | 7.18 |
| 2 | 1 → 3 | 3.91 | 5.02 | 6.07 | 15.01 |
| 2 | 1 → 4 | 6.09 | 4.98 | 3.93 | 14.99 |
| 3 | 1 → 3 | 5.96 | 7.45 | 9.39 | 22.81 |
| 3 | 1 → 4 | 9.04 | 7.55 | 5.61 | 22.19 |
| 4 | 1 → 3 | 5.92 | 7.44 | 9.32 | 22.68 |
| 4 | 1 → 4 | 9.08 | 7.56 | 5.68 | 22.32 |
| 4 | 3 → 5 | 2.12 | 2.6 | 3.1 | 7.82 |
| 4 | 4 → 5 | 2.88 | 2.4 | 1.9 | 7.18 |
| 5 | 1 → 3 | 6.2 | 7.2 | 9.54 | 22.93 |
| 5 | 1 → 4 | 8.8 | 7.8 | 5.46 | 22.07 |
| 5 | 3 → 5 | 3.91 | 5.02 | 6.07 | 15.01 |
| 5 | 4 → 5 | 6.09 | 4.98 | 3.93 | 14.99 |
| 6 | 1 → 3 | 4.15 | 4.76 | 6.22 | 15.13 |
| 6 | 1 → 4 | 5.85 | 5.24 | 3.78 | 14.87 |
| 6 | 3 → 5 | 5.96 | 7.45 | 9.39 | 22.81 |
| 6 | 4 → 5 | 9.04 | 7.55 | 5.61 | 22.19 |
| 7 | 1 → 3 | 2.08 | 2.17 | 3.19 | 7.44 |
| 7 | 1 → 4 | 2.92 | 2.83 | 1.81 | 7.56 |
| 7 | 3 → 5 | 5.92 | 7.44 | 9.32 | 22.68 |
| 7 | 4 → 5 | 9.08 | 7.56 | 5.68 | 22.32 |
| 7 | 5 → 6 | 3.48 | 3.01 | 2.7 | 9.2 |
| 7 | 5 → 7 | 1.52 | 1.99 | 2.3 | 5.8 |
| 8 | 3 → 5 | 6.2 | 7.2 | 9.54 | 22.93 |
| 8 | 4 → 5 | 8.8 | 7.8 | 5.46 | 22.07 |
| 8 | 5 → 6 | 6.58 | 6.16 | 5.22 | 17.96 |
| 8 | 5 → 7 | 3.42 | 3.84 | 4.78 | 12.04 |
| 9 | 3 → 5 | 4.15 | 4.76 | 6.22 | 15.13 |
| 9 | 4 → 5 | 5.85 | 5.24 | 3.78 | 14.87 |
| 9 | 5 → 6 | 10.11 | 8.88 | 7.47 | 26.46 |
| 9 | 5 → 7 | 4.89 | 6.12 | 7.53 | 18.54 |
| 10 | 3 → 5 | 2.08 | 2.17 | 3.19 | 7.44 |
| 10 | 4 → 5 | 2.92 | 2.83 | 1.81 | 7.56 |
| 10 | 5 → 6 | 10.17 | 8.58 | 7.28 | 26.02 |
| 10 | 5 → 7 | 4.83 | 6.42 | 7.72 | 18.98 |
| 10 | 6 → 2 | 3.48 | 3.01 | 2.7 | 9.2 |
| 10 | 7 → 2 | 1.52 | 1.99 | 2.3 | 5.8 |
| 11 | 5 → 6 | 10.31 | 8.06 | 7.19 | 25.55 |
| 11 | 5 → 7 | 4.69 | 6.94 | 7.81 | 19.45 |
| 11 | 6 → 2 | 6.58 | 6.16 | 5.22 | 17.96 |
| 11 | 7 → 2 | 3.42 | 3.84 | 4.78 | 12.04 |
| 12 | 5 → 6 | 6.78 | 5.33 | 4.94 | 17.05 |
| 12 | 5 → 7 | 3.22 | 4.67 | 5.06 | 12.95 |
| 12 | 6 → 2 | 10.11 | 8.88 | 7.47 | 26.46 |
| 12 | 7 → 2 | 4.89 | 6.12 | 7.53 | 18.54 |
| 13 | 5 → 6 | 3.24 | 2.63 | 2.43 | 8.3 |
| 13 | 5 → 7 | 1.76 | 2.37 | 2.57 | 6.7 |
| 13 | 6 → 2 | 10.17 | 8.58 | 7.28 | 26.02 |
| 13 | 7 → 2 | 4.83 | 6.42 | 7.72 | 18.98 |
| 14 | 6 → 2 | 10.31 | 8.06 | 7.19 | 25.55 |
| 14 | 7 → 2 | 4.69 | 6.94 | 7.81 | 19.45 |
| 15 | 6 → 2 | 6.78 | 5.33 | 4.94 | 17.05 |
| 15 | 7 → 2 | 3.22 | 4.67 | 5.06 | 12.95 |
| 16 | 6 → 2 | 3.24 | 2.63 | 2.43 | 8.3 |
| 16 | 7 → 2 | 1.76 | 2.37 | 2.57 | 6.7 |